Title

TNF-α+ CD4+ T cells dominate the SARS-CoV-2 specific T cell response in COVID-19 outpatients and are associated with durable antibodies

Journal

Cell Reports Medicine, 3(6)

ISSN

2666-3791

Authors

van der Ploeg, Kattria
Kirosingh, Adam S
Mori, Diego AM
et al.

Publication Date

2022-06-01

DOI

10.1016/j.xcrm.2022.100640

Peer reviewed

Cell Reports
Medicine

Article

TNF-α^+ CD4$^+$ T cells dominate the SARS-CoV-2 specific T cell response in COVID-19 outpatients and are associated with durable antibodies

Graphical abstract

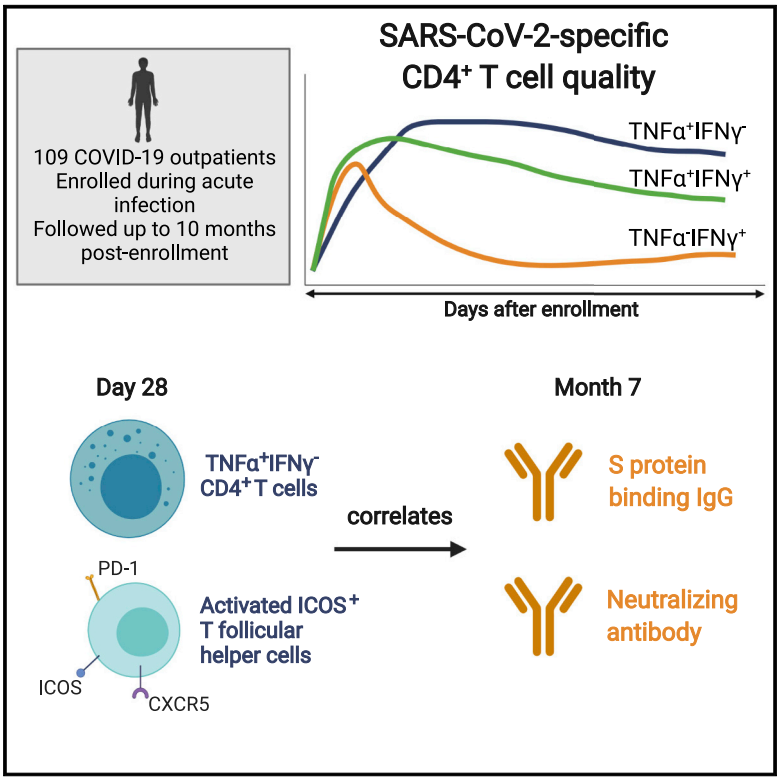

Highlights

- SARS-CoV-2-specific CD4$^+$ response shifts from cells producing IFNγ to TNF-α
- SARS-CoV-2-specific IFNγ^-TNF-α^+ CD4$^+$ T cells predominate at later timepoints
- IFNγ^-TNF-α^+ CD4$^+$ T cells correlate with durable SARS-CoV-2-neutralizing antibodies
- Post-infection mRNA vaccination boosts both IFNγ^+ and TNF-α^+ S-specific CD4$^+$ T cells

Authors

Kattria van der Ploeg, Adam S. Kirosingh, Diego A.M. Mori, ..., Upinder Singh, Taia T. Wang, Prasanna Jagannathan

Correspondence

prasj@stanford.edu

In brief

Van der Ploeg et al. provide a better understanding of CD4$^+$ T cell longitudinal dynamics following SARS-CoV-2 infection and specific features that correlate with the maintenance of neutralizing antibodies. Their data suggest that SARS-CoV-2-specific, TNF-α-producing CD4$^+$ T cells may play an important role in antibody maintenance following COVID-19.

van der Ploeg et al., 2022, Cell Reports Medicine 3, 100640
June 21, 2022
https://doi.org/10.1016/j.xcrm.2022.100640

CellPress

Cell Reports Medicine

CellPress
OPEN ACCESS

Article

TNF-α^+ CD4$^+$ T cells dominate the SARS-CoV-2 specific T cell response in COVID-19 outpatients and are associated with durable antibodies

Kattria van der Ploeg,[1] Adam S. Kirosingh,[2,10] Diego A.M. Mori,[1,10] Saborni Chakraborty,[1,10] Zicheng Hu,[3,4] Benjamin L. Sievers,[5] Karen B. Jacobson,[1] Hector Bonilla,[1] Julie Parsonnet,[1,6] Jason R. Andrews,[1] Kathleen D. Press,[1] Maureen C. Ty,[1] Daniel R. Ruiz-Betancourt,[1] Lauren de la Parte,[1] Gene S. Tan,[5,7] Catherine A. Blish,[1,8] Saki Takahashi,[9] Isabel Rodriguez-Barraquer,[9] Bryan Greenhouse,[8,9] Upinder Singh,[1,2] Taia T. Wang,[1,2] and Prasanna Jagannathan[1,2,11,*]

[1]Department of Medicine, Stanford University School of Medicine, Stanford, CA 94305, USA
[2]Department of Microbiology and Immunology, Stanford University, Stanford, CA 94305, USA
[3]Department of Microbiology and Immunology, University of California San Francisco, San Francisco, CA 94143, USA
[4]Bakar Computational Health Sciences Institute, University of California San Francisco, San Francisco, CA 94143, USA
[5]J. Craig Venter Institute, La Jolla, CA 92037, USA
[6]Department of Epidemiology and Population Health, Stanford University, Stanford, CA 94305, USA
[7]Division of Infectious Disease, Department of Medicine, University of California San Diego, La Jolla, CA 92093, USA
[8]Chan Zuckerberg Biohub, San Francisco, CA 94158, USA
[9]Department of Medicine, University of California San Francisco, San Francisco, CA 94143, USA
[10]These authors contributed equally
[11]Lead contact
*Correspondence: prasj@stanford.edu
https://doi.org/10.1016/j.xcrm.2022.100640

SUMMARY

Severe acute respiratory syndrome coronavirus 2 (SARS-CoV-2)-specific CD4$^+$ T cells are likely important in immunity against coronavirus 2019 (COVID-19), but our understanding of CD4$^+$ longitudinal dynamics following infection and of specific features that correlate with the maintenance of neutralizing antibodies remains limited. Here, we characterize SARS-CoV-2-specific CD4$^+$ T cells in a longitudinal cohort of 109 COVID-19 outpatients enrolled during acute infection. The quality of the SARS-CoV-2-specific CD4$^+$ response shifts from cells producing interferon gamma (IFNγ) to tumor necrosis factor alpha (TNF-α) from 5 days to 4 months post-enrollment, with IFNγ^-IL-21$^-$TNF-α^+ CD4$^+$ T cells the predominant population detected at later time points. Greater percentages of IFNγ^-IL-21$^-$TNF-α^+ CD4$^+$ T cells on day 28 correlate with SARS-CoV-2-neutralizing antibodies measured 7 months post-infection ($\rho = 0.4$, $p = 0.01$). mRNA vaccination following SARS-CoV-2 infection boosts both IFNγ- and TNF-α-producing, spike-protein-specific CD4$^+$ T cells. These data suggest that SARS-CoV-2-specific, TNF-α-producing CD4$^+$ T cells may play an important role in antibody maintenance following COVID-19.

INTRODUCTION

Severe acute respiratory syndrome coronavirus 2 (SARS-CoV-2) has caused hundreds of millions of cases of coronavirus disease 2019 (COVID-19) worldwide, resulting in more than 5 million deaths. Following primary infection or vaccination, individuals generate an adaptive immune response consisting of SARS-CoV-2-specific antibodies, B cells, and T cells; the emergence of this response is associated with successful resolution of COVID-19 symptoms.[1–3] This adaptive immune memory response is likely also critical in protecting individuals against re-infection. Following both infection and vaccination, waning titers of neutralizing antibodies strongly correlate with a risk of re-infection.[4,5] Although several studies have identified long-lived memory immune responses in individuals following infection and vaccination,[6–13] more comprehensive, longitudinal analyses are limited.[14–16] A better understanding of how the quality of SARS-CoV-2-specific memory immune responses changes over time and which features correlate with durable antibodies is key for understanding long-lived immunity to SARS-CoV-2.

Most COVID-19 vaccine development has focused on the generation of neutralizing SARS-CoV-2-specific antibodies,[17,18] given their clinical utility when given via passive transfer[19] and their association with protection against infection.[20–22] SARS-CoV-2-specific CD4$^+$ T cell responses are likely critical to the generation of these antibodies because long-term humoral immunity is dependent on CD4$^+$ T cell help.[23,24] SARS-CoV-2-specific CD4$^+$ T cell responses are more dominant than CD8$^+$ T cell responses[2,13,25] and have been associated with milder disease in acute and convalescent COVID-19 patients,[25–28] suggesting that this response may also play an important role in controlling and resolving a primary SARS-CoV-2 infection.

SARS-CoV-2-specific CD4+ Th1 cells, producing interferon gamma (IFNγ), tumor necrosis factor alpha (TNF-α), and/or interleukin-2 (IL-2), have been identified,[2,25,27,29–31] suggesting an important role for polyfunctional T helper type 1 (Th1) cells in the antiviral response, analogous to other viral infectious diseases.[32] Besides Th1 cells, virus-specific CD4+ T cells also differentiate into T follicular helper (Tfh) cells to instruct B cells, by producing IL-21, for instance, to develop long-term humoral immunity.[23,24,33,34] Circulating Tfh (cTfh) cells have been identified following acute SARS-CoV-2 infection,[10,12,25,27,35–39] although their formation may be delayed,[35] and their relationship with the antibody response remains unclear. Studying the relationship between different CD4+ T cell responses detected following infection, and which responses most strongly correlate with maintenance of antibody responses following infection, is critical toward the development of next-generation vaccines.

To date, most SARS-CoV-2-specific T cell studies have been limited by either small sample size, assessing acute and convalescent samples in different individuals, and/or by evaluating correlations between SARS-CoV-2-specific CD4+ T cell responses and SARS-CoV-2-specific antibody titers measured at concurrent, rather than prospective, time points. To better evaluate the quality of the antigen-specific CD4+ T cell response following infection and to determine whether antigen-specific cTfh cells or other Th populations correlate with durable neutralizing antibodies following infection, we characterized the SARS-CoV-2-specific T cell response over time in a longitudinal cohort of 109 COVID-19 outpatients. Individuals were enrolled within 3 days of PCR-based diagnosis and sampled repeatedly at multiple time points out to 10 months post-enrollment. Moreover, a subset of participants received both doses of mRNA vaccination during follow up, enabling us to evaluate SARS-CoV-2-specific T cell responses in previously infected individuals following vaccination. Our data provide insight into the shifting quality of the SARS-CoV-2-specific CD4+ T cell response following infection and how this is impacted by vaccination. We further identify SARS-CoV-2-specific CD4+ T cell features that are most strongly correlated with neutralizing antibodies. Collectively, our data suggest an important role of SARS-CoV-2-specific, TNF-α-producing CD4+ T cells in antibody maintenance following COVID-19.

RESULTS

SARS-CoV-2-specific CD4+ T cells produce IFNγ, TNF-α, and IL-21 alone or in combination, with TNF-α-producing cells the dominant population

Peripheral blood mononuclear cells (PBMCs) were obtained from 109 COVID-19 outpatients enrolled in a phase 2 trial of Peginterferon Lambda-1a (Lambda) at enrollment (day 0) and 5, 14, 28, and 120 days post-enrollment. The median age of participants was 37 years, 59% were male, and the median duration of symptoms prior to enrollment was 5 days (interquartile range [IQR] 4–7 days; Table S1). Following enrollment, participants completed a daily at-home symptom questionnaire, with a median duration until symptom resolution of 8 days following enrollment.[40] As previously described, two participant groups were identified based on symptom-trajectory analysis, with one cluster (n = 7/109 [6.4%]) characterized by greater symptom severity and/or later peak severity, especially chest pain/pressure, fatigue, and myalgias, and the other cluster characterized by more mild symptoms.[41]

We first investigated the magnitude and quality of SARS-CoV-2-specific T cell responses on day 28 post-enrollment using intracellular cytokine staining (ICS). PBMCs were stimulated with two PepTivator SARS-CoV-2 peptide pools: membrane glycoprotein and nucleocapsid phosphoprotein, pooled together (MN), or spike (S) protein, and assessed for intracellular production of IFNγ, TNF-α, IL-10, and IL-21. Antigen-specific CD4+ T cells were identified by first gating on non-naïve CD4+ T cells (excluding CCR7+CD45RA+ CD4+ T cells; Figures 1A and S1A). As we detected no antigen-specific CD4+ T cell production of IL-10 (Figure S1C), downstream analyses focused on IFNγ, TNF-α, and IL-21. We found that SARS-CoV-2-specific CD4+ T cells consist of four distinct cytokine-producing populations: TNF-α alone (IFNγ−IL-21−TNF-α+), IFNγ alone (IFNγ+IL-21−TNF-α−), IL-21 alone (IFNγ−IL-21+TNF-α−), or both IFNγ and TNF-α (IFNγ+IL-21−TNF-α+), with the highest percentages of cells being IFNγ−IL-21−TNF-α+ (Figures 1B and S1C). In separate experiments, we found that the majority of IFNγ−IL-21−TNF-α+ and IFNγ+IL-21−TNF-α+ CD4+ T cells also co-produce IL-2 (Figure S2). Percentages of MN-specific IFNγ−IL-21−TNF-α+, IFNγ+IL-21−TNF-α−, and IFNγ+IL-21−TNF-α+ cells were slightly greater compared with S-protein-specific cells (Figure 1B). When considering the quality of the SARS-CoV-2-specific CD4+ T cell response (e.g., the proportion of antigen-specific cells making specific cytokines, alone or in combination), >50% of the MN- and S-specific CD4+ T cell response was comprised of IFNγ−IL-21−TNF-α+ cells (Figure 1B). CD4+ T cells producing TNF-α alone were significantly higher in males compared with females, older participants (>35 years of age), and those experiencing greater symptom severity and/or later peak severity as previously defined[41] (Figure S3), consistent with published reports.[7,14] SARS-CoV-2-specific CD8+ T cells were overall low and heterogeneous, with a few high responders (Figures S4A and S4B), and less abundant than SARS-CoV-2-specific CD4+ T cells in this ICS assay, consistent with other reports.[13,25] No significant differences in cytokine-producing SARS-CoV-2-specific CD4+ or CD8+ T cells were observed between Peginterferon Lambda and placebo treatment arms (Figures S5A and S5B). Together, these data suggest that SARS-CoV-specific IFNγ−IL-21−TNF-α+ CD4+ T cells are the dominant population detected 28 days post-enrollment in this outpatient cohort and that their magnitude is influenced by participant gender, age, and disease severity.

As an alternate approach to ICS, we also performed an activation-induced marker (AIM) assay to assess SARS-CoV-2-specific CD4+ T cells via upregulation of CD137 and OX40 (Figure S1B).[2,7,27,42] In contrast to responses characterized by ICS, we observed similar percentages of AIM+ CD4+ T cells following MN- and S-protein stimulation (Figure 1D). In addition, similar percentages of AIM+ cells were found between CD4+ and CD8+ T cells following MN stimulation (Figures S1C, S4C, and S4D). As with the ICS assay, responses were similar between Lambda and placebo treatment arms in SARS-CoV-2-specific AIM+ CD4+ and CD8+ T cell responses and in SARS-CoV-2 full-length S-binding immunoglobulin G (IgG) or

CellPress
OPEN ACCESS

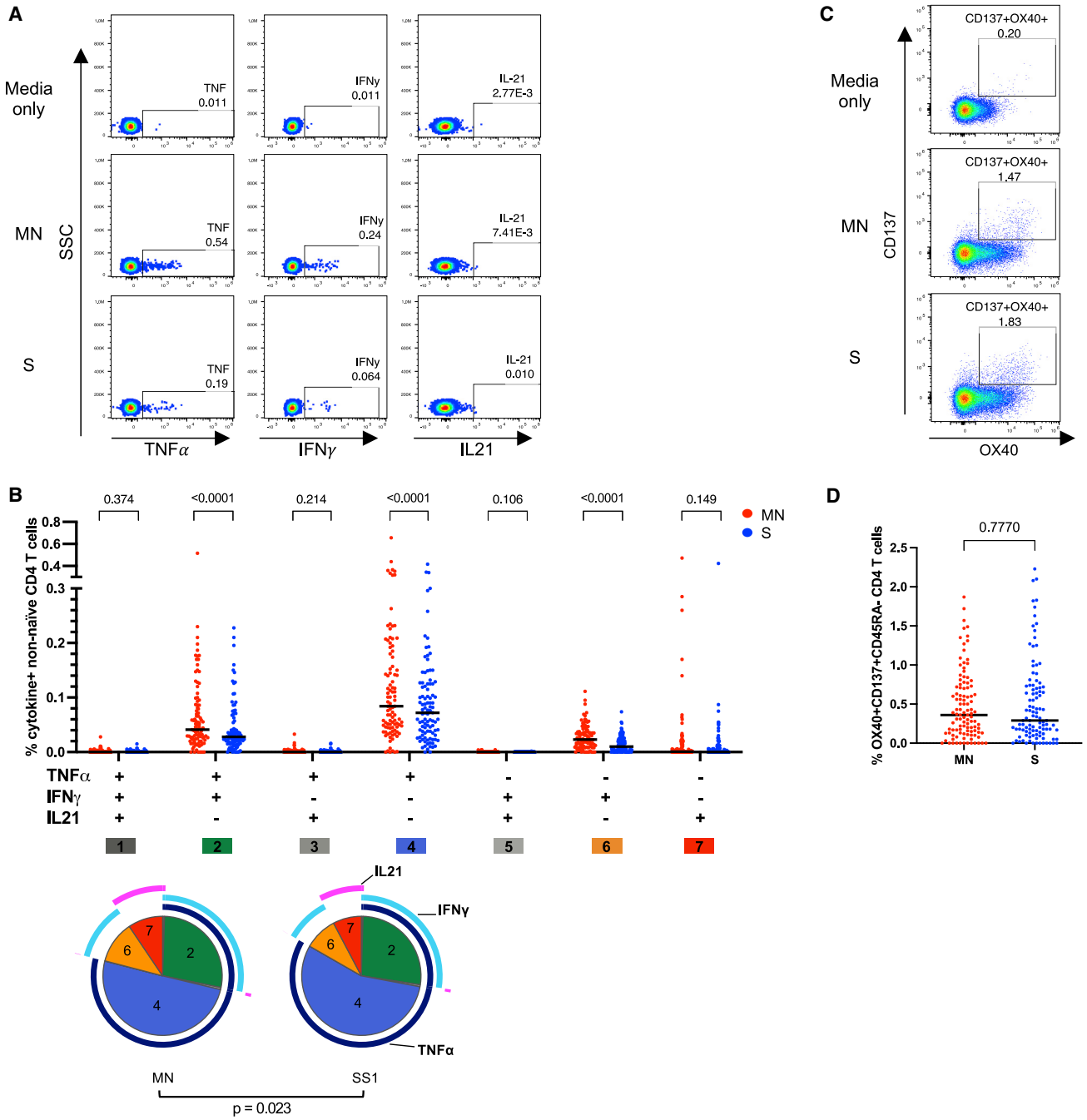

Figure 1. Identification of four distinct SARS-CoV-2-specific CD4⁺ T cell subsets that differ between S- and MN-protein stimulation

PBMCs of COVID-19 outpatients on day 28 post-enrollment were stimulated with spike (S) or a combination of membrane (M) and nucleocapsid (N) proteins *in vitro* and were stained and analyzed by flow cytometry.

(A and C) Representative flow plots of (A) cytokine-producing (TNF-α, IFNγ, and IL-21) or (C) AIM-expressing ($CD137^+OX40^+$) $CD45RA^-$ $CD4^+$ T cells that are stimulated with "media only" or MN or S proteins.

(B) The absolute percentage (scatterplot; black line, median) of each individual combination of TNF-α-, IFNγ-, and IL-21-producing non-naïve $CD4^+$ T cells stratified by antigenic stimuli (red: MN, blue: S; n = 99). The pie charts show the relative proportion (mean) of each individual combination of cytokine-producing non-naïve $CD4^+$ T cells (e.g., pie slice 4 represents $TNF\text{-}\alpha^+IFN\gamma^{--}IL\text{-}21^{--}$) among the total population of antigen-specific cells, stratified by antigenic stimuli (MN: n = 102, S: n = 100). The p value shown under the pie charts is calculated using a partial permutation test.

(D) Shown are absolute percentages of $OX40^+CD137^+$ $CD45RA^-$ $CD4^+$ T cells stratified by antigenic stimuli with the black line indicating the median (n = 104).

(B and D) p values shown above the scatterplots are calculated using Wilcoxon matched-pairs signed rank test. Values shown are background (media-only condition) subtracted.

See also Figures S1–S3 and S5.

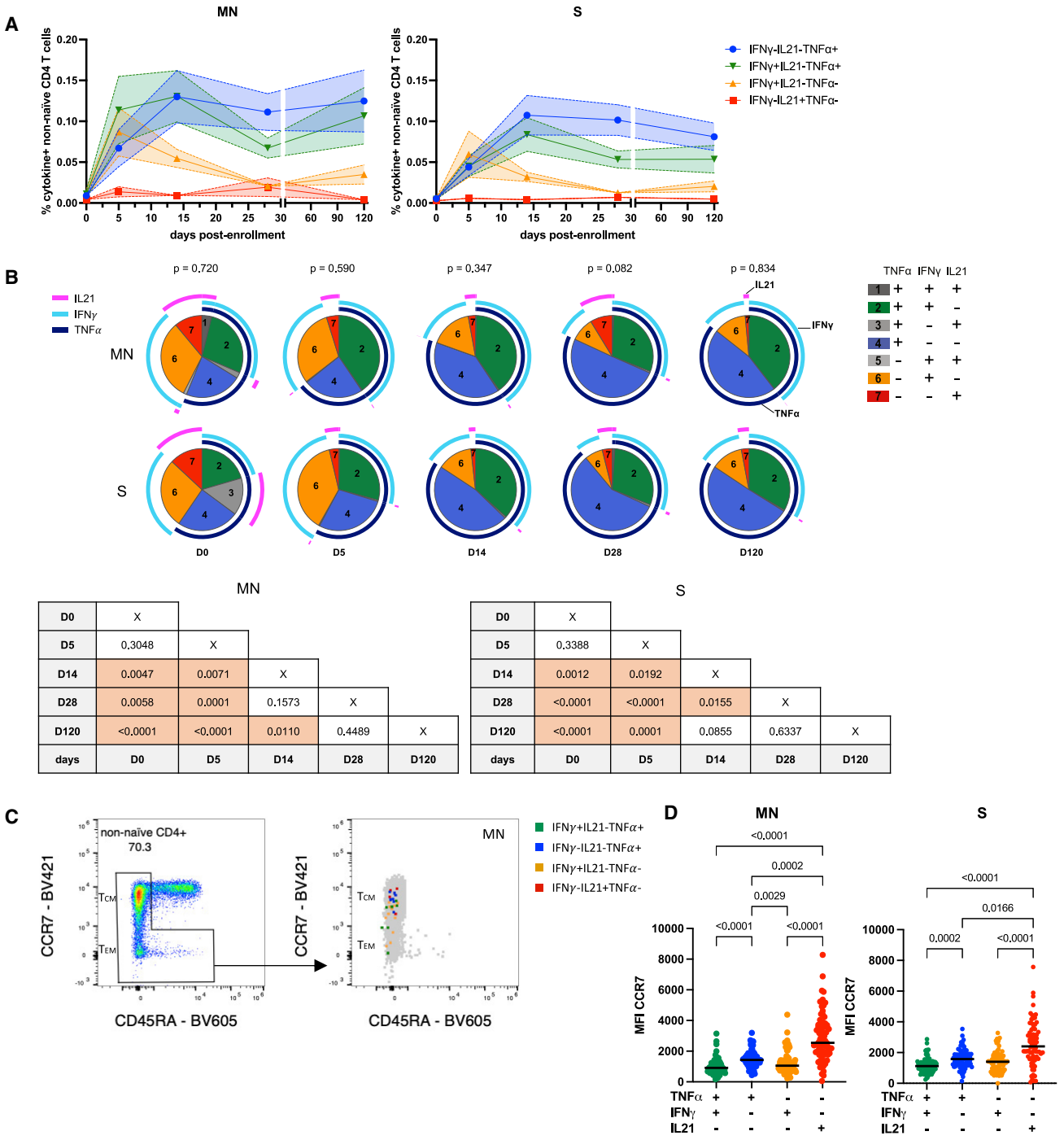

MN					
D0	X				
D5	0.3048	X			
D14	0.0047	0.0071	X		
D28	0.0058	0.0001	0.1573	X	
D120	<0.0001	<0.0001	0.0110	0.4489	X
days	D0	D5	D14	D28	D120

S					
D0	X				
D5	0.3388	X			
D14	0.0012	0.0192	X		
D28	<0.0001	<0.0001	0.0155	X	
D120	<0.0001	0.0001	0.0855	0.6337	X
days	D0	D5	D14	D28	D120

Figure 2. Kinetics of four distinct cytokine-producing SARS-CoV-2-specific CD4$^+$ T cell populations over time and the density of CCR7 receptor expression on these populations

(A and B) PBMCs from 24 COVID-19 outpatients sampled at days 5, 14, and 28 and month 4 (day 120) (n = 10 also sampled on day of enrollment [day 0]) were stimulated with MN (left) or S (right) proteins *in vitro* and were stained and analyzed by flow cytometry.

(A) The mean and SEM of the absolute percentage of background-subtracted IFNγ^-IL-21$^-$TNF-α^+- (blue), IFNγ^+IL-21$^-$TNF-α^-- (yellow), IFNγ^-IL-21$^+$TNF-α^-- (red), or IFNγ^+IL-21$^-$TNF-α^+-producing non-naïve CD4$^+$ T cells (green) of sequential timepoints post-enrollment are shown. These four populations were the dominant populations identified in Figure 1.

(B) The relative proportion of each individual combination of background-subtracted, TNF-α-, IFN-γ, and IL-21-producing non-naïve CD4$^+$ T cells stratified by sequential days are depicted in the pie charts (mean). The p values indicated on top of the pie charts are calculated using the partial permutation test, which tests the association between MN- and S-protein stimulation of each indicated day post-enrollment. The p values in the tables indicate the significance of

(legend continued on next page)

neutralizing-antibody titers measured on day 28 post-enrollment (Figures S5C–S5E). Altogether, these data suggest that a single dose of Peginterferon Lambda treatment did not have a measurable impact on the adaptive immune response 28 days post-treatment.

Longitudinal analysis suggests a shift in quality of SARS-CoV-2-specific CD4$^+$ T cell response from predominantly IFNγ to TNF-α over time

We next investigated the magnitude and quality of the SARS-CoV-2-specific T cell response by ICS over time, starting from the day of enrollment (day 0) until month 4 (day 120) post-enrollment in the same individuals. On day five, MN-specific CD4$^+$ T cells primarily produced both IFNγ and TNF-α, and S-specific cells primarily produced IFNγ alone (Figures 2A, 2B, and S6A). At day 14, we observed a shift in the quality of the MN- and S-protein-specific T cell response, with significant increases in the magnitude and proportion of IFNγ$^-$IL-21$^-$TNF-α$^+$ CD4$^+$ T cells. These TNF-α-producing CD4$^+$ T cells were the predominant population of SARS-CoV-2-specific CD4$^+$ detected up to 4 months after enrollment, while the percentage of IFNγ-producing CD4$^+$ T cells declined over time. The magnitude of SARS-CoV-2-specific IFNγ$^-$IL-21$^+$TNF-α$^-$ CD4$^+$ T cells was low (Figures 2A, 2B, and S6A). This changing quality of CD4$^+$ T cells was observed following both MN- and S-protein stimulation (Figure 2B). Similar results were observed when analyzing T cell responses considering days since symptom onset (rather than days since enrollment) (Figures S6B–S6D), as well as when analyzing samples from the Lambda and placebo arms separately (Figures S5D and S5F). Among non-naïve cytokine-producing CD8$^+$ T cells, IFNγ$^+$IL-21$^-$TNF-α$^-$ cells were the predominant population up to day 28, followed by IFNγ$^+$IL-21$^-$TNF-α$^+$ cells at 4 months post-enrollment. These findings were driven by a few high responders, which were particularly observed after MN stimulation (Figures S4E and S4F).

To further characterize CD4$^+$ IFNγ$^+$ and TNF-α$^+$ cells, we examined CCR7 cell-surface-receptor expression to better understand their differentiation status (e.g., central versus effector memory). SARS-CoV-2-specific IFNγ$^-$IL-21$^-$TNFα$^+$ CD4$^+$ T cells had a significantly higher CCR7 mean fluorescence intensity compared with IFNγ$^+$IL-21$^-$TNF-α$^-$ or IFNγ$^+$IL-21$^-$TNF-α$^+$ cells (Figures 2C and 2D). This suggests that CD4$^+$ T cells producing TNF-α alone were more central-memory-like, while the IFNγ-producing populations were more effector-memory-like. Together, these data suggest a shift in the magnitude and quality of the SARS-CoV-2-specific CD4$^+$ T cell response over time with a switch from an IFNγ-producing, effector-memory-like response at early time points to a TNF-α-producing, central-memory-like response at later time points.

Activated cTfh, SARS-CoV-2-specific cTfh, and AIM$^+$ CD4$^+$ T cell percentages correlate with SARS-CoV-2-specific TNF-α and IFNγ cytokine-producing CD4$^+$ T cells

We next profiled other CD4$^+$ T cell populations longitudinally, including SARS-CoV-2-specific AIM$^+$ (CD137$^+$OX40$^+$) CD4$^+$, cTfh (PD-1$^+$CXCR5$^+$CD4$^+$), activated cTfh (ICOS$^+$), and SARS-CoV-2-specific AIM$^+$ cTfh (PD-1$^+$CXCR5$^+$OX40$^+$CD137$^+$) cells (Figures 3B and S1B for gating). We observed similar percentages of SARS-CoV-2-specific AIM$^+$ CD4$^+$ T cells between days 5 and 28, although both MN- and S-protein-specific AIM$^+$ CD4$^+$ declined between days 28 and 120 (Figure 3A). In general, the cTfh percentage remained similar over time with the exception of a greater percentage of cTfh cells on day 5 compared with day 28 (Figure 3C). Activated cTfh percentage declined after day 14 (Figure 3D). SARS-CoV-2-specific AIM$^+$ cTfh cells were detectable up to 4 months after enrollment, and magnitudes remained largely unchanged over time (Figure 3E).

Subsequently, we assessed the relationship between production of cytokines and expression of activation markers, specifically investigating correlations between (1) SARS-CoV-2-specific cytokine-producing CD4$^+$ T cell percentages measured in ICS experiments and (2) percentages of SARS-CoV-2-specific AIM$^+$ CD4$^+$ and the three different cTfh populations measured in the AIM assays, because it is unclear how these T cell populations relate to each other. All IFNγ- and TNF-α-producing CD4$^+$ T cell populations positively and significantly correlated with AIM$^+$ CD4$^+$, AIM$^+$ cTfh, and ICOS$^+$ cTfh cells. In contrast, IFNγ$^-$IL-21$^+$TNF-α$^-$ CD4$^+$ T cells did not correlate with circulating percentages of cTfh cells (Figures 3F and 3G). Together, these data suggest that SARS-CoV-2-specific TNF-α- and IFNγ-producing CD4$^+$ T cell populations highly correlated with SARS-CoV-2-specific AIM$^+$ CD4$^+$ T cell and cTfh cell populations, but that, in our assay, IL-21 production did not correlate with either AIM$^+$ or cTfh cell populations.

SARS-CoV-2-specific TNF-α$^+$ CD4 T cell and activated cTfh cell responses on day 28 correlate with durable antibody responses

Neutralizing antibodies are thought to be the primary adaptive effector function that mediate protection from COVID-19 re-infection.[20–22] CD4$^+$ T helper responses are important in germinal center immune reactions and affinity maturation, and antigen-specific cTfh cells were recently described to be a correlate of the peak antibody response following SARS-CoV-2 vaccination.[9] We thus explored whether specific CD4$^+$ T cell features following natural infection correlated with the antibody response measured at time points in the future, including S-protein-binding IgG and neutralizing antibody titers (Figure S5D).[43]

the associations between the different days post-enrollment calculated using the partial permutation test (left: MN-protein-stimulated T cells; right: S-protein-stimulated T cells).
(C) Representative flow cytometry plots of CCR7- and CD45RA-expressing CD4$^+$ T cells (left) with an overlay of MN-protein-specific IFNγ$^-$IL-21$^-$TNF-α$^+$- (blue), IFNγ$^+$IL-21$^-$TNF-α$^-$- (yellow), IFNγ$^-$IL-21$^+$TNF-α$^-$-(red), or IFNγ$^+$IL-21$^-$TNF-α$^+$-producing non-naïve CD4$^+$ T cells (green, right).
(D) Mean fluorescence intensity (MFI) of CCR7 on MN- (left, n = 72) or S-protein-specific (right, n = 74) single positive TNF-α- (blue), IFNγ- (yellow), IL-21- (red), or TNF-α- and IFNγ-producing non-naïve CD4$^+$ T cells (green) from day 28 post-enrollment.
The p values were calculated using the Friedman test with Dunn's multiple comparisons test (black line, median).
See also Figures S1, S2, and S4–S6.

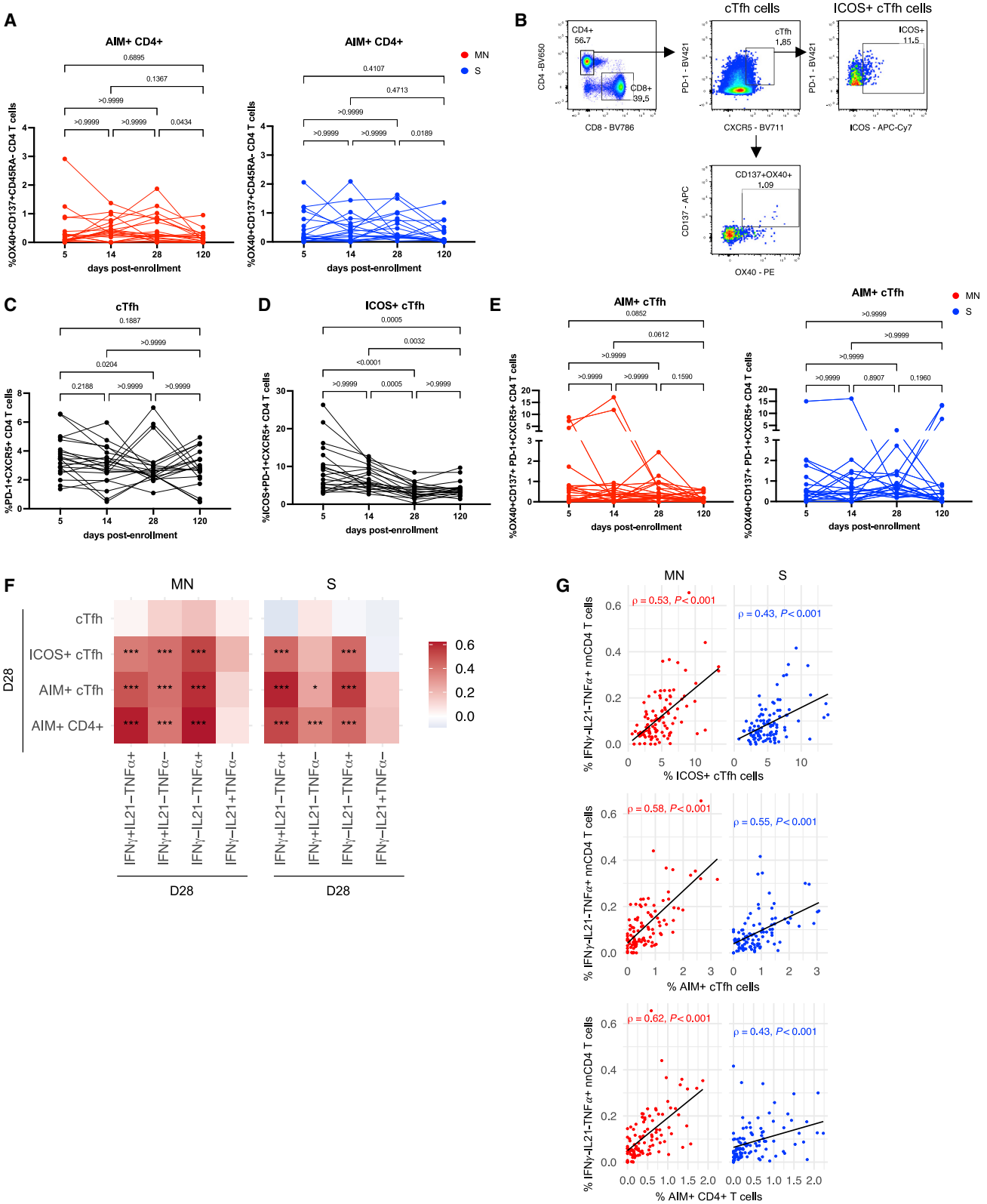

(legend on next page)

We first evaluated whether SARS-CoV-2-specific CD4$^+$ T cell responses measured early following infection (day 5) correlated with the peak antibody response, measured on day 28 post-enrollment.[43,44] MN-protein-specific, IFNγ^+-producing responses measured on day 5 positively correlated with S-protein-binding IgG on day 28, although this correlation was not significant after multiple comparison correction (Figures 4A, 4B, S7A, and S7B). Furthermore, percentages of antigen-specific cTfh cells, and other CD4$^+$ T cell populations, measured on day 5 were also not significantly correlated with SARS-CoV-2-specific antibody responses measured on day 28 (Figure 4A).

We next examined whether SARS-CoV-2-specific CD4$^+$ T cell responses measured later (day 28) were associated with the durability of the antibody response, assessing correlations with antibody responses measured at day 28 and month 7 (day 210). After multiple comparison correction, we found that SARS-CoV-2-specific CD4$^+$ T cells that produce TNF-α, in particular IFNγ^-IL-21$^-$TNF-α$^+$ cells, and activated, ICOS$^+$ cTfh cells on day 28, correlated significantly and positively with both S-binding IgG and neutralizing antibody titers measured on days 28 and 210 (Figures 4C–4E). Results were similar when analyzing the Lambda and placebo arms separately (Figures S5G and S5H). In linear models adjusted for treatment arm, gender, and age, associations between MN-protein-specific $\log_{10}$ IFNγ^-IL-21$^-$TNF-α$^+$-producing CD4$^+$ T cells and antibody responses on day 210 remained significant (Table 1). Similarly, associations between ICOS$^+$ cTfh cells on day 28 and antibody responses on day 210 remained significant after multivariate adjustment (Table 1). We observed similar positive correlations when analyzing associations between month 4 (day 120) T cell responses and day 210 antibody responses, particularly after MN stimulation, but these associations were not significant, likely given the small sample size at month 4 (Figures S7C and S7D). Taken together, these findings show that SARS-CoV-2-specific IFNγ^-IL-21$^-$TNF-α$^+$ CD4$^+$ T cells and activated, ICOS$^+$ cTfh cells on day 28 correlate with SARS-CoV-2-specific antibody responses measured more than 7 months post-infection.

Early proteomic and transcriptomic signatures associate with T cell responses on day 28 post-enrollment

Given the robust associations between SARS-CoV-2-specific IFNγ^-IL-21$^-$TNF-α$^+$ CD4$^+$ T cells and ICOS$^+$ cTfh cells, and durable neutralizing antibody titers, we next sought to identify early, infection-induced determinants of this response. We performed whole-blood RNA sequencing and plasma proteomics by Olink on days 0 and 5 post-enrollment[45] and correlated these measurements with the day 28 SARS-CoV-2-specific CD4$^+$ T cell response (Figure 5A). Several transcriptomic pathways associated with B cell activation, including B cell-mediated immunity pathways, B cell receptor signaling, and immunoglobulin production, were associated with both SARS-CoV-2-specific CD4$^+$ T cells producing IFNγ^-IL-21$^-$TNF-α$^+$ and activated, ICOS$^+$ cTfh cells measured on day 28 (Figures 5A and 5C). In addition, higher levels of several plasma proteins measured on days 0 and 5 post-enrollment were associated with greater percentages of SARS-CoV-2-specific CD4$^+$ T cell responses measured on day 28, including IFNγ^-IL-21$^-$TNF-α$^+$-producing cells (Figure 5A; Table S2) and ICOS$^+$ cTfh cells (Figure 5C; Table S3). Several of these proteins were associated with both cellular populations, including monocyte-chemotactic protein 3 (MCP-3, also known as CCL7), eukaryotic translation initiation factor 4 gamma 1 (EIF4G1), DNA fragmentation factor subunit alpha (DFFA), and C-X-C motif chemokine ligand 1 (CXCL1) (Figures 5B and 5D). MCP-3 is a cytokine induced by IFNγ and acts as a chemoattractant for activated leukocytes including CCR2$^+$ monocytes.[46,47] Although elevated levels of MCP3 have previously been implicated in the pathogenesis of severe COVID-19,[45,48,49] our data suggest that it may also be a useful early biomarker for the initiation of a robust, long-lived adaptive cellular immune response.

SARS-CoV-2-specific CD4$^+$ T cells producing IFNγ and TNF-α and AIM$^+$ cTfh cells are boosted following COVID-19 mRNA vaccination

COVID-19 vaccines elicit robust humoral and CD4$^+$ T cell responses among participants who had not been previously exposed to SARS-CoV-2.[50–53] However, little has been reported to date on the CD4$^+$ T cell response following mRNA vaccination among individuals who have experienced SARS-COV-2 infection.[8,9] We evaluated the SARS-CoV-2-specific CD4$^+$ T cell response in study participants who received two doses of a COVID-19 mRNA vaccine either prior to month 7 (n = 2) or 10 (n = 18) follow-up visits and compared these changes with

Figure 3. The kinetics of SARS-CoV-2-specific AIM$^+$ CD4$^+$, activated cTfh, and SARS-CoV-2-specific cTfh cell percentages and their correlation with cytokine-producing CD4$^+$ T cells

PBMCs of COVID-19 outpatients on days 5, 14, 28, and 120 post-enrollment were stimulated with MN or S proteins *in vitro* and were stained and analyzed by flow cytometry.

(A) The kinetics of the absolute percentage of paired MN- (left, n = 22) or S- (right, n = 19) protein-stimulated AIM$^+$ CD45RA$^-$ CD4$^+$ T cells over time.

(B) The gating strategy of PD-1$^+$CXCR5$^+$CD4$^+$ (cTfh), PD-1$^+$CXCR5$^+$ICOS$^+$CD4$^+$ (ICOS$^+$ cTfh), and PD-1$^+$CXCR5$^+$OX40$^+$CD137$^+$CD4$^+$ (AIM$^+$ cTfh) cells.

(C and D) The kinetics of the absolute percentage of paired (C) cTfh (n = 21) and (D) ICOS$^+$ cTfh (n = 21) cells of unstimulated cells (media only) are depicted.

(E) The kinetics of the absolute percentage paired AIM$^+$ cTfh cells stimulated with MN (left, n = 22) or S (right, n = 19) protein over time are shown.

(A and C–E) The p values were calculated using the Friedman test with Dunn's multiple comparisons test.

(F) The heatmap shown depicts Spearman's correlations (Benjamini-Hochberg corrected) between the percentages of MN- (left, n = 101) or S-protein-stimulated (right, n = 100) cTfh cell populations (cTfh, ICOS$^+$ cTfh, and AIM$^+$ cTfh) or AIM$^+$ CD45RA$^-$ CD4$^+$ T cells measured in AIM experiments and cytokine-producing non-naïve CD4$^+$ T cells measured in ICS experiments. The measurements that are significantly associated are indicated by asterisks (*p < 0.05, ***p < 0.001). The scale bar indicates the Spearman's correlation rho (ρ).

(G) Scatterplots comparing antigen-stimulated (MN: left/red, n = 101; S: right/blue, n = 100) IFNγ^-IL-21$^-$TNF-α$^+$-producing T cells with ICOS$^+$ cTfh (top), AIM$^+$ cTfh (middle), or AIM$^+$ CD45RA$^-$ CD4$^+$ T (bottom) cells are shown (n = 101).

The rho (ρ) and p values were calculated using Spearman's correlation (Benjamini-Hochberg corrected). The lines represent the fitted linear relationship between the indicated cell populations.

See also Figure S1.

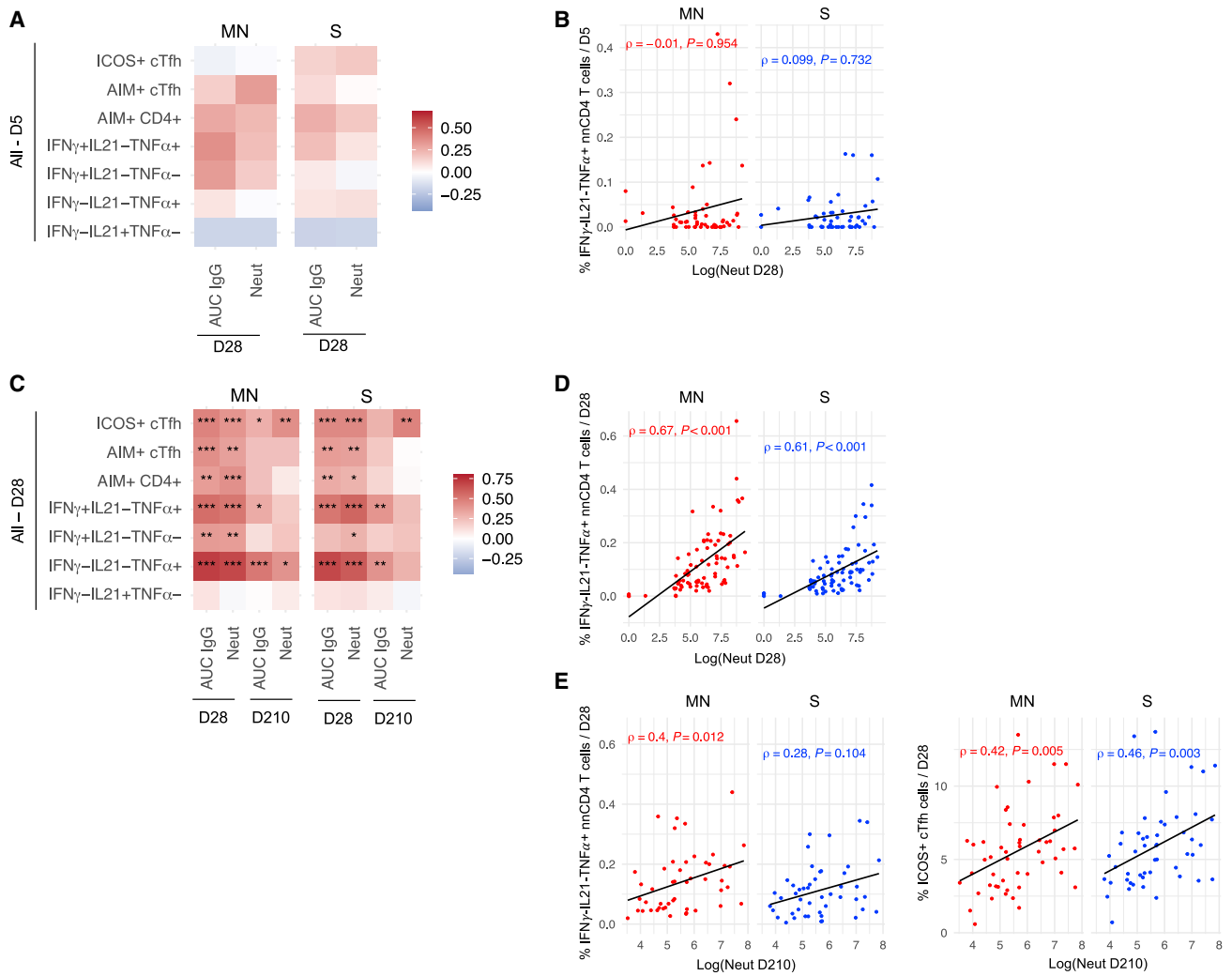

Figure 4. Late T cell responses are positively correlated with durability of antibody titers, while early T cell responses are not associated with the peak magnitude of antibody titers

(A and C) In the heatmaps, Spearman's correlations (Benjamini-Hochberg corrected) between indicated cTfh cell populations, AIM^+ $CD45RA^-$ $CD4^+$, and $cytokine^+$ non-naïve $CD4^+$ T cell data and antibody titers (S protein IgG binding [area under the curve (AUC) IgG] or neutralizing antibody (Neut) are shown. The measurements that are significantly associated are indicated by asterisks (*p < 0.05, **p < 0.01, ***p < 0.001). The scale bar indicates the Spearman's correlation rho (ρ).

(A) Correlations are performed between indicated T cell data collected at day 5 post-enrollment and indicated antibody titers at day 28 post-enrollment.

(B) Scatterplots comparing MN- (left/red) and S-protein-stimulated (right/blue) $IFN\gamma^-IL\text{-}21^-TNF\text{-}\alpha^+$-producing non-naïve $CD4^+$ T cells collected on day 5 (MN: n = 55; S: n = 51) post-enrollment with neutralizing antibody titers collected on day 28 post-enrollment are depicted.

(C) Correlations are performed between indicated T cell data collected on day 28 post-enrollment and indicated antibody titers at day 28 or 210 post-enrollment.

(D) Scatterplots comparing antigen-stimulated $IFN\gamma^-IL\text{-}21^-TNF\text{-}\alpha^+$-producing non-naïve $CD4^+$ T cells collected on day 28 (MN: n = 81; S: n = 78) post-enrollment with neutralizing antibody titers collected on day 28 post-enrollment are shown.

(E) Scatterplots comparing antigen-stimulated $IFN\gamma^-IL\text{-}21^-TNF\text{-}\alpha^+$-producing non-naïve $CD4^+$ T cells (left, MN: n = 48, S: n = 47) or $ICOS^+$ cTfh cells (right, MN: n = 52, S: n = 50) collected on day 28 with neutralizing antibody titers collected on day 210 post-enrollment are shown.

(B, D, and E) The neutralizing antibody titers are presented in natural logarithm, and we added +1 to allow for inclusion of participants with no neutralizing activity. The rho (ρ) and p values were calculated using Spearman's correlation (Benjamini-Hochberg corrected). The lines represent the fitted linear relationship between the indicated data.

See also Figures S5 and S7.

unvaccinated participants. As expected, we found that the magnitude of S-protein-specific, but not MN-protein-specific, $IFN\gamma^+IL\text{-}21^-TNF\text{-}\alpha^-$- and $IFN\gamma^+IL\text{-}21^-TNF\text{-}\alpha^+$-producing $CD4^+$ T cells was increased in the post-vaccination samples only (Figures 6A and S8A). The month 10/day 28 ratio of S-protein-specific $IFN\gamma^+IL\text{-}21^-TNF\text{-}\alpha^-$ cells was 3.3-fold higher, and for $IFN\gamma^+IL\text{-}21^-TNF\text{-}\alpha^+$ cells was 4.9-fold higher, comparing vaccinated with unvaccinated participants. In contrast, we observed

Table 1. Linear model calculating associations between SARS-CoV-2-specific CD4+ T cell populations measured at day 28 and antibody responses measured at day 210

	Unadjusted		Adjusted[a]	
Day 28 CD4+ T cell populations	Coef (95% CI)	p value	Coef (95% CI)	p value
MN-specific nnCD4+				
Log10 IFNγ-IL-21-TNF-α+	0.63 (0.17–1.10)	0.009	0.59 (0.10–1.07)	0.02
Log10 IFNγ+IL-21-TNF-α+	0.22 (-0.17–0.60)	0.25	0.17 (-0.27–0.60)	0.44
Log10 AIM + CD4+	0.23 (-0.32–0.76)	0.41	0.24 (-0.33–0.82)	0.40
Log10 ICOS + cTfh	0.86 (0.34–1.38)	0.002	0.83 (0.28–1.38)	0.004
Log10 AIM + cTfh	0.38 (-0.08–0.83)	0.10	0.38 (-0.10–0.85)	0.12
S-specific nnCD4+				
Log10 IFNγ-IL-21-TNF-α+	0.35 (-0.10–0.78)	0.12	0.22 (-0.24–0.68)	0.33
Log10 IFNγ+IL-21-TNF-α+	0.31 (-0.07–0.69)	0.11	0.19 (-0.23–0.61)	0.36
Log10 AIM + CD4+	0.12 (-0.34–0.58)	0.59	0.08 (-0.40–0.55)	0.73
Log10 ICOS + cTfh	0.96 (0.38–1.54)	0.002	0.92 (0.30–1.54)	0.005
Log10 AIM + cTfh	0.27 (-0.19–0.73)	0.25	0.24 (-0.25–0.73)	0.33

[a]Adjusted for treatment arm, gender, and age.

a more modest, 1.4-fold increase in the month 10/day 28 ratio of S-protein-specific IFNγ-IL-21-TNF-α+ cells (Figure 6B). These differences did not appear to be driven by time since second dose (Figure S8B). Additionally, vaccinated individuals had a 4.3-fold higher month 10/day 28 ratio of S-protein-specific AIM+ cTfh cells compared with unvaccinated participants (Figure 6C), without boosting of AIM+ CD4+ T cells or activated cTfh cells (Figures S8C and S8D). Together, these findings show that mRNA vaccination boosted S-protein-specific CD4+ T cells that produced IFNγ, with or without TNF-α, along with AIM+ cTfh cells.

DISCUSSION

In this longitudinal study of SARS-CoV-2-specific CD4+ T cell magnitude and quality in outpatients enrolled in a phase 2 clinical trial of Peginterferon Lambda, we identified a shift in the quality of the SARS-CoV-2-specific CD4+ T cell response from an IFNγ-producing response at early time points to a TNF-α-producing response at later time points (≥day 28). IFNγ-IL-21-TNF-α+ CD4+ T cells were the predominant cytokine-producing T cell population following infection and sustained up to month 10 post-enrollment. Percentages of TNF-α-producing CD4+ T cells were positively correlated with AIM+ T cell populations and activated, ICOS+ cTfh cells. Higher percentages of TNF-α-producing CD4+ T cells and ICOS+ cTfh cells were more commonly found in participants who had experienced a more severe infection and were positively associated with higher levels of the chemokine CCL7/MCP-3 at the time of enrollment. Percentages of IFNγ-IL-21-TNF-α+CD4+ T cells, along with activated, ICOS+ cTfh cells, were positively correlated with neutralizing antibodies measured up to 7 months post-enrollment. These cells were only modestly boosted following mRNA vaccination compared with other cellular populations, including S-protein-specific AIM+ cTfh cells and IFNγ+-producing CD4+ T cells.

Polyfunctional CD4+ Th1 cells producing IFNγ and TNF-α (along with IL-2) have been thought to be important in response to some viral infections, including HIV and influenza.[32,54,55] This polyfunctional Th1 cytokine profile has been observed among convalescent mild and severe COVID-19 patient in several studies,[2,6,13,25,27,29–31,39] although the importance of this versus other cytokine-producing populations of circulating SARS-CoV-2-specific CD4+ T cells remains unclear. However, many of these studies were cross-sectional in nature, with significant heterogeneity observed.[11,25,27,28,31] In the present study, we detected a substantial proportion of CD4+ T cells producing both IFNγ and TNF-α (along with IL-2) that peaked in percentage early in convalescence. In contrast, at later time points, TNF-α-producing cells, without IFNγ, were the predominant population detected in our ICS assay. This finding is particularly relevant given the development of clinical assays designed to detect SARS-CoV-2-specific T cell responses via measurement of IFNγ release[56] and suggests that assays measuring SARS-CoV-2-specific TNF-α production, and/or IL-2 production,[57] could be considered a tool to define previous exposure to SARS-CoV-2.

In addition to measuring SARS-CoV-2-specific T cells by ICS, we also utilized an AIM assay employing markers for both CD4+ T cells and cTfh cells and, similar to published reports,[7,15] detected SARS-CoV-2-specific AIM+ CD4+ T cells up to 10 months post-enrollment. Moreover, we observed that cytokine-producing CD4+ T cell populations—in particular, TNF-α single positive cells—positively and significantly correlated with AIM+ CD4+ T cells, activated ICOS+ cTfh cells, and AIM+ cTfh cells. Given their central-memory-like phenotype, we speculate that SARS-CoV-2-specific TNF-α single positive cells may represent a memory pool of either memory Th1 or Tfh cells[58] or stem-cell-like memory cells;[15] molecular work is ongoing to identify transcription factors that might help elucidate the ontogeny of these cells. Our observations that several plasma proteins, including the chemokine MCP-3/CCL7, measured at the time of infection strongly correlate with higher percentages of these cells on day 28 suggest that a robust innate immune response at the

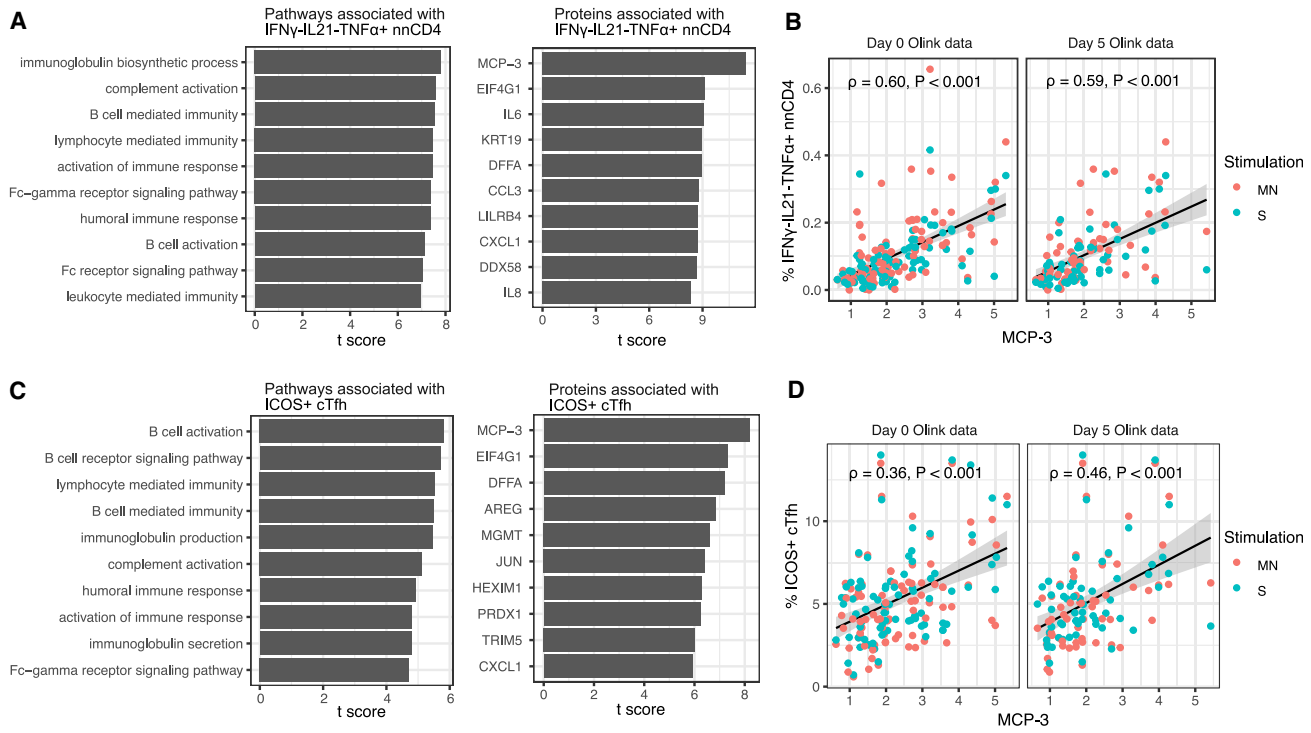

Figure 5. Associations between early immune response and T cell responses on day 28 post-enrollment

(A) Gene-Ontology-based immune pathways (left) and plasma proteins (right) associated with the absolute percentage of SARS-CoV-2-specific IFNγ$^-$IL-21$^-$TNF-α$^+$ non-naïve CD4$^+$ T cells on day 28.

(B) Scatterplots showing associations between the MCP-3 on day 0 or 5 and the percentage of SARS-CoV-2-specific IFNγ$^-$IL-21-TNF-α$^+$ non-naïve CD4$^+$ T cells on day 28.

(C) Gene-Ontology-based immune pathways (left) and plasma proteins (right) associated with the absolute percentage of ICOS$^+$ cTfh cells on day 28.

(D) Scatterplots showing associations between the MCP-3 on day 0 or 5 and ICOS$^+$ cTfh cells on day 28.

(A and C) We used regression models to test the association while controlling for the sampling time of immune pathways or proteins (day 0 or 5) and the stimulation type (MN or S) of the T cell response.

(B and D) The color of the points represents the stimulating antigens. The spearman correlations (rho [ρ]) between MCP-3 and the T cell percentages and the corresponding p values are reported.

See also Tables S2 and S3.

time of infection may lead to greater expansion of this cell subset; however, this immune activation may also represent a double-edged sword given its association with early disease progression.[45,48,49] No correlation was observed between IL-21-producing CD4$^+$ T cells and cTfh cells. This was unexpected given that IL-21 is thought to be a canonical cTfh cell cytokine.[23,24,33,34] Furthermore, we were unable to detect any antigen-specific IL-10 production. One possible explanation for these findings is that our ICS assay was not optimized to detect SARS-CoV-2-specific IL-21 or IL-10 production, although we and others have successfully used a similar approach to detect these CD4$^+$ T cell cytokines in other settings.[59] Alternatively, it is possible that cTfh cells are not representative of germinal center Tfh cells in this setting or that these cytokines may not be induced in the SARS-CoV-2-specific CD4$^+$ T cell compartment following infection, although this will require further validation in other cohorts and settings.

Although several studies have reported correlations between SARS-CoV-2-specific CD4$^+$ T cell responses and SARS-CoV-2-specific antibody titers measured at either the peak of response or at concurrent timepoints,[7,13,27,30,35,60] there is limited data correlating infection-induced CD4$^+$ T cell responses with antibodies measured prospectively. Although SARS-CoV-2-specific, polyfunctional IFNγ and TNF-α co-producing CD4$^+$ T cells at day 5 correlated with the neutralizing antibody response at day 28 by Spearman correlation, this finding was not significant after multiple comparison correction. In contrast, we observed that TNF-α single positive cells measured on day 28, rather than polyfunctional, IFNγ and TNF-α co-producing cells, were most strongly correlated with neutralizing antibodies measured 7 months post-enrollment. We also observed a significant positive correlation between activated, ICOS$^+$ cTfh cell percentages on day 28 and neutralization antibodies on month 7. This suggests that SARS-CoV-2-specific TNF-α-producing CD4$^+$ T cells and activated cTfh cells measured weeks after infection may serve as a useful correlate to identify individuals who exhibit durable antibodies. Furthermore, additional characterization of these cellular populations would help identify strategies to determine whether boosting of this response could increase durability of neutralizing antibodies.

CellPress
OPEN ACCESS

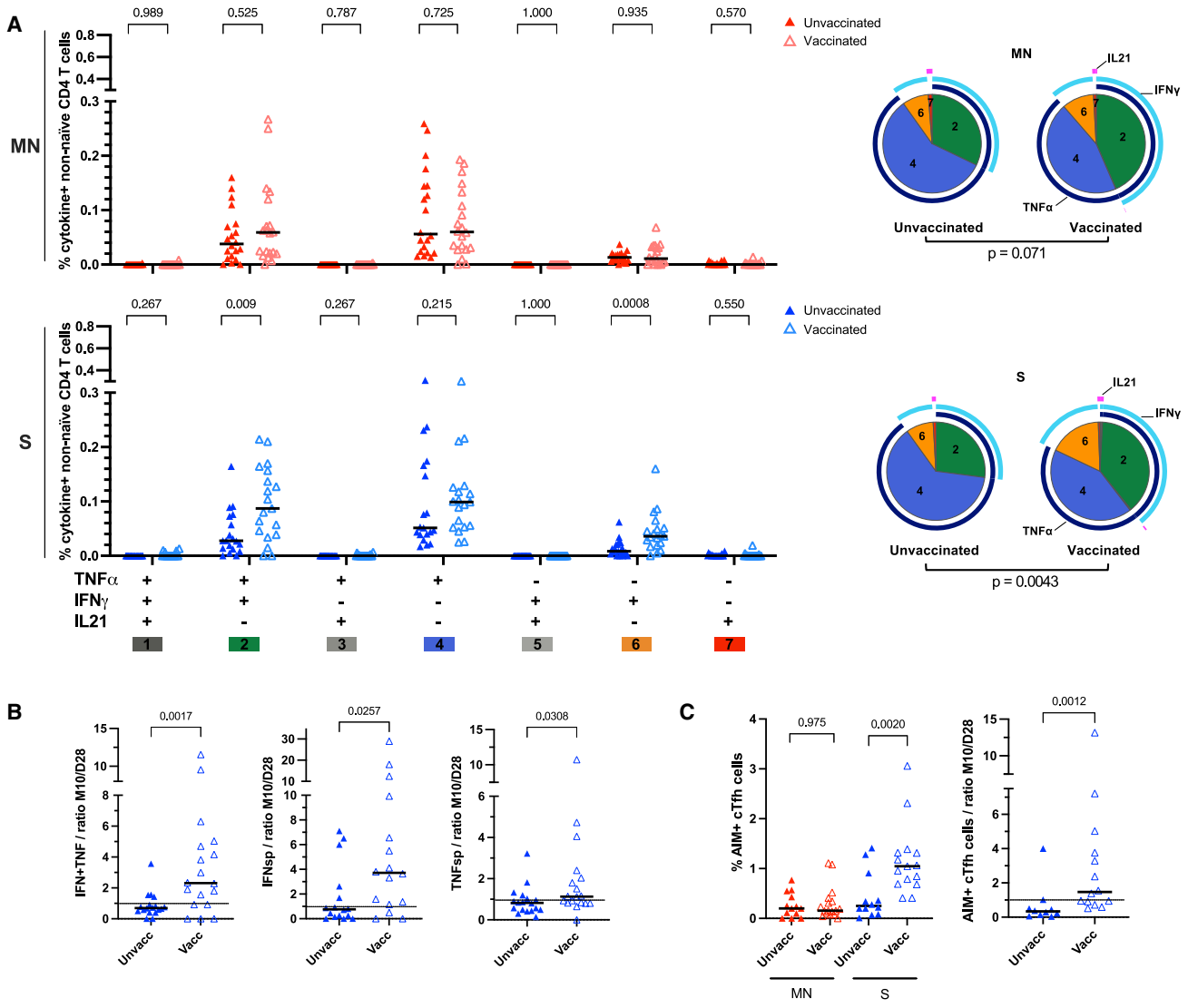

Figure 6. mRNA vaccination boosts IFNγ$^+$IL-21$^-$TNF-α$^-$- and IFNγ$^+$IL-21$^-$TNF-α$^+$-producing CD4$^+$ T cells and AIM$^+$ cTfh cells

PBMCs of COVID-19 outpatients on month 10 post-enrollment were stimulated with S or MN proteins *in vitro* and were stained and analyzed by flow cytometry.

(A) The absolute percentage (scatterplot; black line, median) of each individual combination of TNF-α-, IFNγ-, and IL-21-producing non-naïve CD4$^+$ T cells stratified by vaccination status (closed triangle: unvaccinated, n = 20; open triangle: vaccinated, n = 20). Top panel depicts MN-protein-stimulated CD4$^+$ T cells (red), and bottom panel depicts S-protein-stimulated CD4$^+$ T cells (blue). p values shown above the scatterplots are calculated using the Mann Whitney test. The pie charts show the relative proportion (mean) of each individual combination of cytokine-producing non-naïve CD4$^+$ T cells (e.g., pie slice 4 represents TNFa$^+$IFNγ$^-$IL-21$^-$) among the total populaton of antigen-specifc cells, stratified by antigenic stimuli. The p value shown under the pie charts is calculated using a partial permutation test.

(B) The ratio between month 10 and day 20 of the absolute percentage of IFNγ$^+$IL-21$^-$TNF-α$^+$- (IFN + TNF, left), IFNγ$^+$IL-21$^-$TNF-α$^-$- (IFNsp, middle), or IFNγ$^-$IL-21$^-$TNF-α$^+$-producing (TNFsp, right) non-naïve CD4$^+$ T cells stimulated with the S protein is depicted (scatterplot; black line, median).

(C) The absolute percentage (left) and the ratio between month 10 and day 28 of AIM$^+$ (CD137$^+$/OX40$^+$) cTfh cells (right) stimulated with the MN (red) or S (blue) proteins and stratified by vaccination status are shown.

(B and C) The p values shown are calculated using the Mann Whitney test. See also Figure S8.

Given our study design, we were positioned to compare CD4$^+$ T cell responses among previously infected study participants who did and did not receive two doses of a COVID-19 mRNA vaccine during follow up. We found that mRNA vaccination particularly boosts S-protein-specific CD4$^+$ T cells that produce IFNγ, with or without TNF-α, along with AIM$^+$ cTfh cells. There was only modest boosting of TNF-α single positive cells and no boosting of MN-protein-specific cells. These findings are consistent with a recent systems analysis of immune responses following the BNT162b2 mRNA vaccine.[61] In that study, Arunachalam and colleagues found that vaccination resulted in robust expansion of IFNγ-producing CD4$^+$ T cells, although they observed no significant correlation between levels of IFNγ-producing CD4$^+$ T cells and the neutralizing antibody response

measured prospectively. In another study by Painter and colleagues, the percentage of antigen-specific cTfh cells prior to the second dose of mRNA vaccination correlated with post-second dose neutralizing antibody titers. In contrast, pre-second dose antigen-specific Th1 cells were less well correlated, suggesting distinct associations between Th populations and vaccine-elicited immune responses.[9] Together, these data suggest that the quality of the $CD4^+$ T cell response differs between natural infection and vaccination, although the downstream impact of different $CD4^+$ T cell responses on the neutralizing antibody response and protective immunity remain unclear.

By providing insight into the shifting quality of the SARS-CoV-2-specific $CD4^+$ T cell response following infection, how this is impacted by vaccination, and which features most strongly correlate with immune effector mechanisms, our study adds to our growing understanding of the memory T cell response to SARS-CoV-2. Given ongoing SARS-CoV-2 transmission and increasing risk of both re-infections and breakthrough infections following vaccination, identification of correlates of protective immunity remains critical in the design of next-generation COVID-19 vaccination strategies.

Limitations of the study

This study had some limitations. Half of the study participants in this trial received an investigational type III IFN at the time of infection. However, in our study, this agent neither shortened the duration of viral shedding nor symptoms,[40] nor did we observe any significant impact on either innate[45] or adaptive immune responses between arms (Figure S5), allowing us to utilize data from both arms to improve statistical power. Furthermore, stratified analyses, and multivariate models adjusted for treatment arm as a covariate, confirmed pooled results, though this may differ in alternative study populations. We would have liked to have assessed for correlations with protection against re-infection; however, only one participant had evidence of re-infection during follow up. Future larger cohorts, and/or case/control designs, will be required to address this question. Next, analysis of T cell cytokine production was only performed by an ICS assay. Although SARS-CoV-2-specific $CD8^+$ T cells were low and less abundant than $CD4^+$ T cells in the ICS assay, consistent with published reports,[13,25] similar percentages of antigen-specific $CD8^+$ and $CD4^+$ T cells were detected by an AIM assay, raising the question of whether ICS adequately detects the cytokines being produced. ICS using alternative cytokines, longer stimulation periods, and/or alternative methods for cytokine detection (e.g., ELISpot or single-cell RNA sequencing) should be performed to validate these results. Finally, we only utilized data assessing responses to the original consensus strain and do not present data on the responses to variants. However, others have recently reported that infection-induced SARS-CoV-2 T cell responses have broad reactivity against viral variant proteins.[62,63]

STAR★METHODS

Detailed methods are provided in the online version of this paper and include the following:

SUPPLEMENTAL INFORMATION

Supplemental information can be found online at https://doi.org/10.1016/j.xcrm.2022.100640.

ACKNOWLEDGMENTS

This study was supported by NIH/NIAID (U01 AI150741-01S1 to Z.H., S.T., I.R.-B., B.G., T.T.W., and P.J.), the Stanford's Innovative Medicines Accelerator, and a Fastgrant (to C.A.B.). The Lambda clinical trial was funded by anonymous donors to Stanford University, and Peginterferon Lambda was provided by Eiger BioPharmaceuticals. The funders had no role in data collection and analysis or the decision to publish. We thank all study participants who participated in this study, the study team for their tireless work, and Thanmayi Ranganath, Nancy Q. Zhao, Aaron J. Wilk, Rosemary Vergara, Julia L. McKechnie, Giovanny J. Martínez-Colón, Arjun Rustagi, Geoff Ivison, Ruoxi Pi, Madeline J. Lee, Taylor Hollis, Georgie Nahass, Kazim Haider, and Laura Simpson for assistance with processing samples. We also thank our colleagues at Stanford University Occupational Health and at San Mateo Medical Center for participant referrals. The Stanford REDCap platform (http://redcap.stanford.edu) is developed and operated by the Stanford Medicine Research IT team. The REDCap platform services at Stanford are subsidized by the (1) Stanford School of Medicine Research Office and (2) the National Center for Research Resources and the National Center for Advancing Translational Sciences, National Institutes of Health, through grant UL1 TR001085. The graphical abstract was created with BioRender.com.

AUTHOR CONTRIBUTIONS

Conceptualization, K.v.d.P., A.S.K., S.C., Z.H., B.L.S., J.P., J.R.A., U.S., T.T.W., and P.J.; methodology, K.v.d.P., A.S.K., S.C., Z.H., B.L.S., J.R.A., G.S.T., C.A.B., S.T., I.R.-B., B.G., T.T.W., and P.J.; formal analysis, K.v.d.P., A.S.K., S.C., Z.H., and P.J.; investigation, K.v.d.P., D.A.M.M., S.C., B.L.S., K.B.J., H.B., J.P., J.R.A., K.D.P., M.C.T., D.R.R.-B., L.d.l.P., G.S.T., C.A.B., U.S., T.T.W., and P.J.; data curation, K.v.d.P., D.A.M.M., S.C., B.L.S., K.B.J., K.D.P., M.C.T., D.R.R.-B., L.d.l.P., C.A.B., U.S., T.T.W., and P.J.; visualization, K.v.d.P.; supervision, P.J.; project administration, D.A.M.M. and P.J.; funding acquisition, C.A.B., B.G., U.S., T.T.W., and P.J.; writing – original draft, K.v.d.P. and P.J.; writing – review & editing, all authors.

DECLARATION OF INTERESTS

The authors declare no competing interests.

INCLUSION AND DIVERSITY

We worked to ensure gender balance in the recruitment of human subjects. We worked to ensure ethnic or other types of diversity in the recruitment of human subjects. One or more of the authors of this paper self-identifies as an underrepresented ethnic minority in science. One or more of the authors of this paper self-identifies as a member of the LGBTQ+ community.

Received: January 26, 2022
Revised: March 26, 2022
Accepted: April 27, 2022
Published: May 3, 2022

REFERENCES

1. Chen, Z., and John Wherry, E. (2020). T cell responses in patients with COVID-19. Nat. Rev. Immunol. *20*, 529–536. https://doi.org/10.1038/s41577-020-0402-6.
2. Grifoni, A., Weiskopf, D., Ramirez, S.I., Mateus, J., Dan, J.M., Moderbacher, C.R., Rawlings, S.A., Sutherland, A., Premkumar, L., Jadi, R.S., et al. (2020). Targets of T Cell responses to SARS-CoV-2 coronavirus in humans with COVID-19 disease and unexposed individuals. Cell *181*, 1489–1501. https://doi.org/10.1016/j.cell.2020.05.015.
3. Sette, A., and Crotty, S. (2021). Adaptive immunity to SARS-CoV-2 and COVID-19. Cell *184*, 861–880. https://doi.org/10.1016/j.cell.2021.01.007.
4. Anand, S., Montez-Rath, M.E., Han, J., Garcia, P., Cadden, L., Hunsader, P., Kerschmann, R., Beyer, P., Boyd, S.D., Chertow, G.M., and Parsonnet, J. (2021). Serial SARS-CoV-2 receptor-binding domain antibody responses in patients receiving dialysis. Ann. Intern. Med. *174*, 1073–1080. https://doi.org/10.7326/m21-0256.
5. Cromer, D., Juno, J.A., Khoury, D., Reynaldi, A., Wheatley, A.K., Kent, S.J., and Davenport, M.P. (2021). Prospects for durable immune control of SARS-CoV-2 and prevention of reinfection. Nat. Rev. Immunol. *21*, 395–404. https://doi.org/10.1038/s41577-021-00550-x.
6. Breton, G., Mendoza, P., Hägglöf, T., Oliveira, T.Y., Schaefer-Babajew, D., Gaebler, C., Turroja, M., Hurley, A., Caskey, M., and Nussenzweig, M.C. (2021). Persistent cellular immunity to SARS-CoV-2 infection. J. Exp. Med. *218*, e20202515. https://doi.org/10.1084/jem.20202515.
7. Dan, J.M., Mateus, J., Kato, Y., Hastie, K.M., Yu, E.D., Faliti, C.E., Grifoni, A., Ramirez, S.I., Haupt, S., Frazier, A., et al. (2021). Immunological memory to SARS-CoV-2 assessed for up to 8 months after infection. Science *371*, eabf4063. https://doi.org/10.1126/science.abf4063.
8. Goel, R.R., Painter, M.M., Apostolidis, S.A., Mathew, D., Meng, W., Rosenfeld, A.M., Lundgreen, K.A., Reynaldi, A., Khoury, D.S., Pattekar, A., et al. (2021). mRNA vaccines induce durable immune memory to SARS-CoV-2 and variants of concern. Science *374*, abm0829. https://doi.org/10.1126/science.abm0829.
9. Painter, M.M., Mathew, D., Goel, R.R., Apostolidis, S.A., Pattekar, A., Kuthuru, O., Baxter, A.E., Herati, R.S., Oldridge, D.A., Gouma, S., et al. (2021). Rapid induction of antigen-specific CD4+ T cells is associated with coordinated humoral and cellular immunity to SARS-CoV-2 mRNA vaccination. Immunity *54*, 2133–2142.e3. https://doi.org/10.1016/j.immuni.2021.08.001.
10. Rodda, L.B., Netland, J., Shehata, L., Pruner, K.B., Morawski, P.A., Thouvenel, C.D., Takehara, K.K., Eggenberger, J., Hemann, E.A., Waterman, H.R., et al. (2021). Functional SARS-CoV-2-specific immune memory persists after mild COVID-19. Cell *184*, 169–183.e17. https://doi.org/10.1016/j.cell.2020.11.029.
11. Tan, A.T., Linster, M., Tan, C.W., Le Bert, N., Chia, W.N., Kunasegaran, K., Zhuang, Y., Tham, C.Y.L., Chia, A., Smith, G.J.D., et al. (2021). Early induction of functional SARS-CoV-2-specific T cells associates with rapid viral clearance and mild disease in COVID-19 patients. Cell Rep. *34*, 108728. https://doi.org/10.1016/j.celrep.2021.108728.
12. Wheatley, A.K., Juno, J.A., Wang, J.J., Selva, K.J., Reynaldi, A., Tan, H.-X., Lee, W.S., Wragg, K.M., Kelly, H.G., Esterbauer, R., et al. (2021). Evolution of immune responses to SARS-CoV-2 in mild-moderate COVID-19. Nat. Commun. *12*, 1162. https://doi.org/10.1038/s41467-021-21444-5.
13. Zuo, J., Dowell, A.C., Pearce, H., Verma, K., Long, H.M., Begum, J., Aiano, F., Amin-Chowdhury, Z., Hoschler, K., Brooks, T., et al. (2021). Robust SARS-CoV-2-specific T cell immunity is maintained at 6 months following primary infection. Nat. Immunol. *22*, 620–626. https://doi.org/10.1038/s41590-021-00902-8.
14. Cohen, K.W., Linderman, S.L., Moodie, Z., Czartoski, J., Lai, L., Mantus, G., Norwood, C., Nyhoff, L.E., Edara, V.V., Floyd, K., et al. (2021). Longitudinal analysis shows durable and broad immune memory after SARS-CoV-2 infection with persisting antibody responses and memory B and T cells. Cell Rep. Med. *2*, 100354. https://doi.org/10.1016/j.xcrm.2021.100354.
15. Jung, J.H., Rha, M.-S., Sa, M., Choi, H.K., Jeon, J.H., Seok, H., Park, D.W., Park, S.-H., Jeong, H.W., Choi, W.S., and Shin, E.C. (2021). SARS-CoV-2-specific T cell memory is sustained in COVID-19 convalescent patients for 10 months with successful development of stem cell-like memory T cells. Nat. Commun. *12*, 4043. https://doi.org/10.1038/s41467-021-24377-1.
16. Peluso, M.J., Deitchman, A.N., Torres, L., Iyer, N.S., Munter, S.E., Nixon, C.C., Donatelli, J., Thanh, C., Takahashi, S., Hakim, J., et al. (2021). Long-term SARS-CoV-2-specific immune and inflammatory responses in individuals recovering from COVID-19 with and without post-acute symptoms. Cell Rep *36*, 109518. https://doi.org/10.1016/j.celrep.2021.109518.
17. Corey, L., Mascola, J.R., Fauci, A.S., and Collins, F.S. (2020). A strategic approach to COVID-19 vaccine R&D. Science *368*, 948–950. https://doi.org/10.1126/science.abc5312.
18. Thanh Le, T., Andreadakis, Z., Kumar, A., Gómez Román, R., Tollefsen, S., Saville, M., and Mayhew, S. (2020). The COVID-19 vaccine development landscape. Nat. Rev. Drug Discov. *19*, 305–306. https://doi.org/10.1038/d41573-020-00073-5.
19. Weinreich, D.M., Sivapalasingam, S., Norton, T., Ali, S., Gao, H., Bhore, R., Musser, B.J., Soo, Y., Rofail, D., Im, J., et al. (2021). REGN-COV2, a neutralizing antibody cocktail, in outpatients with covid-19. N. Engl. J. Med. *384*, 238–251. https://doi.org/10.1056/nejmoa2035002.
20. Addetia, A., Crawford, K.H.D., Dingens, A., Zhu, H., Roychoudhury, P., Huang, M.-L., Jerome, K.R., Bloom, J.D., and Greninger, A.L. (2020). Neutralizing antibodies correlate with protection from SARS-CoV-2 in humans during a fishery vessel outbreak with a high attack rate. J. Clin. Microbiol. *58*, e02107-20. https://doi.org/10.1128/jcm.02107-20.
21. Huang, A.T., Garcia-Carreras, B., Hitchings, M.D.T., Yang, B., Katzelnick, L.C., Rattigan, S.M., Borgert, B.A., Moreno, C.A., Solomon, B.D., Trimmer-Smith, L., et al. (2020). A systematic review of antibody mediated immunity to coronaviruses: kinetics, correlates of protection, and association with severity. Nat. Commun. *11*, 4704. https://doi.org/10.1038/s41467-020-18450-4.
22. Khoury, D.S., Cromer, D., Reynaldi, A., Schlub, T.E., Wheatley, A.K., Juno, J.A., Subbarao, K., Kent, S.J., Triccas, J.A., and Davenport, M.P. (2021). Neutralizing antibody levels are highly predictive of immune protection from symptomatic SARS-CoV-2 infection. Nat. Med. *27*, 1205–1211. https://doi.org/10.1038/s41591-021-01377-8.
23. Crotty, S. (2019). T follicular helper cell Biology: a decade of discovery and diseases. Immunity *50*, 1132–1148. https://doi.org/10.1016/j.immuni.2019.04.011.
24. Hale, J.S., and Ahmed, R. (2015). Memory T follicular helper CD4 T cells. Front. Immunol. *6*, 16. https://doi.org/10.3389/fimmu.2015.00016.
25. Sekine, T., Perez-Potti, A., Rivera-Ballesteros, O., Strålin, K., Gorin, J.-B., Olsson, A., Llewellyn-Lacey, S., Kamal, H., Bogdanovic, G., Muschiol, S., et al. (2020). Robust T cell immunity in convalescent individuals with asymptomatic or mild COVID-19. Cell *183*, 158–168. https://doi.org/10.1016/j.cell.2020.08.017.

26. Liao, M., Liu, Y., Yuan, J., Wen, Y., Xu, G., Zhao, J., Cheng, L., Li, J., Wang, X., Wang, F., et al. (2020). Single-cell landscape of bronchoalveolar immune cells in patients with COVID-19. Nat. Med. *26*, 842–844. https://doi.org/10.1038/s41591-020-0901-9.

27. Rydyznski Moderbacher, C., Ramirez, S.I., Dan, J.M., Grifoni, A., Hastie, K.M., Weiskopf, D., Belanger, S., Abbott, R.K., Kim, C., Choi, J., et al. (2020). Antigen-specific adaptive immunity to SARS-CoV-2 in acute COVID-19 and associations with age and disease severity. Cell *183*, 996–1012.e19. https://doi.org/10.1016/j.cell.2020.09.038.

28. Zhou, R., To, K.K.-W., Wong, Y.-C., Liu, L., Zhou, B., Li, X., Huang, H., Mo, Y., Luk, T.-Y., Lau, T.T.-K., et al. (2020). Acute SARS-CoV-2 infection impairs dendritic cell and T cell responses. Immunity *53*, 864–877.e5. https://doi.org/10.1016/j.immuni.2020.07.026.

29. Braun, J., Loyal, L., Frentsch, M., Wendisch, D., Georg, P., Kurth, F., Hippenstiel, S., Dingeldey, M., Kruse, B., Fauchere, F., et al. (2020). SARS-CoV-2-reactive T cells in healthy donors and patients with COVID-19. Nature *587*, 270–274. https://doi.org/10.1038/s41586-020-2598-9.

30. Peng, Y., Mentzer, A.J., Liu, G., Yao, X., Yin, Z., Dong, D., Dejnirattisai, W., Rostron, T., Supasa, P., Liu, C., et al. (2020). Broad and strong memory CD4+ and CD8+ T cells induced by SARS-CoV-2 in UK convalescent individuals following COVID-19. Nat. Immunol. *21*, 1336–1345. https://doi.org/10.1038/s41590-020-0782-6.

31. Weiskopf, D., Schmitz, K.S., Raadsen, M.P., Grifoni, A., Okba, N.M.A., Endeman, H., van den Akker, J.P.C., Molenkamp, R., Koopmans, M.P.G., van Gorp, E.C.M., et al. (2020). Phenotype and kinetics of SARS-CoV-2–specific T cells in COVID-19 patients with acute respiratory distress syndrome. Sci. Immunol. *5*, eabd2071. https://doi.org/10.1126/sciimmunol.abd2071.

32. Seder, R.A., Darrah, P.A., and Roederer, M. (2008). T-cell quality in memory and protection: implications for vaccine design. Nat. Rev. Immunol. *8*, 247–258. https://doi.org/10.1038/nri2274.

33. Eto, D., Lao, C., DiToro, D., Barnett, B., Escobar, T.C., Kageyama, R., Yusuf, I., and Crotty, S. (2011). IL-21 and IL-6 are critical for different aspects of B cell immunity and redundantly induce optimal follicular helper CD4 T cell (Tfh) differentiation. PLoS One *6*, e17739. https://doi.org/10.1371/journal.pone.0017739.

34. Rasheed, M.A.U., Latner, D.R., Aubert, R.D., Gourley, T., Spolski, R., Davis, C.W., Langley, W.A., Ha, S.-J., Ye, L., Sarkar, S., et al. (2013). Interleukin-21 is a critical cytokine for the generation of virus-specific long-lived plasma cells. J. Virol. *87*, 7737–7746. https://doi.org/10.1128/jvi.00063-13.

35. Boppana, S., Qin, K., Files, J.K., Russell, R.M., Stoltz, R., Bibollet-Ruche, F., Bansal, A., Erdmann, N., Hahn, B.H., and Goepfert, P.A. (2021). SARS-CoV-2-specific circulating T follicular helper cells correlate with neutralizing antibodies and increase during early convalescence. PLoS Pathog. *17*, e1009761. https://doi.org/10.1371/journal.ppat.1009761.

36. Gong, F., Dai, Y., Zheng, T., Cheng, L., Zhao, D., Wang, H., Liu, M., Pei, H., Jin, T., Yu, D., and Zhou, P. (2020). Peripheral CD4+ T cell subsets and antibody response in COVID-19 convalescent individuals. J. Clin. Invest. *130*, 6588–6599. https://doi.org/10.1172/jci141054.

37. Juno, J.A., Tan, H.-X., Lee, W.S., Reynaldi, A., Kelly, H.G., Wragg, K., Esterbauer, R., Kent, H.E., Batten, C.J., Mordant, F.L., et al. (2020). Humoral and circulating follicular helper T cell responses in recovered patients with COVID-19. Nat. Med. *26*, 1428–1434. https://doi.org/10.1038/s41591-020-0995-0.

38. Meckiff, B.J., Ramírez-Suástegui, C., Fajardo, V., Chee, S.J., Kusnadi, A., Simon, H., Eschweiler, S., Grifoni, A., Pelosi, E., Weiskopf, D., et al. (2020). Imbalance of regulatory and cytotoxic SARS-CoV-2-reactive CD4+ T cells in COVID-19. Cell *183*, 1340–1353.e16. https://doi.org/10.1016/j.cell.2020.10.001.

39. Neidleman, J., Luo, X., Frouard, J., Xie, G., Gill, G., Stein, E.S., McGregor, M., Ma, T., George, A.F., Kosters, A., et al. (2020). SARS-CoV-2-Specific T cells exhibit phenotypic features of helper function, lack of terminal differentiation, and high proliferation potential. Cell Rep. Med. *1*, 100081. https://doi.org/10.1016/j.xcrm.2020.100081.

40. Jagannathan, P., Andrews, J.R., Bonilla, H., Hedlin, H., Jacobson, K.B., Balasubramanian, V., Purington, N., Kamble, S., de Vries, C.R., Quintero, O., et al. (2021). Peginterferon Lambda-1a for treatment of outpatients with uncomplicated COVID-19: a randomized placebo-controlled trial. Nat. Commun. *12*, 1967. https://doi.org/10.1038/s41467-021-22177-1.

41. Jacobson, K.B., Purington, N., Parsonnet, J., Andrews, J., Balasubramanian, V., Bonilla, H., Edwards, K., Desai, M., Singh, U., Hedlin, H., and Jagannathan, P. (2022). Inflammatory but not respiratory symptoms are associated with ongoing upper airway viral shedding in outpatients with uncomplicated COVID-19. Diagn. Microbiol. Infect. Dis. *102*, 115612. https://doi.org/10.1016/j.diagmicrobio.2021.115612.

42. Reiss, S., Baxter, A.E., Cirelli, K.M., Dan, J.M., Morou, A., Daigneault, A., Brassard, N., Silvestri, G., Routy, J.-P., Havenar-Daughton, C., et al. (2017). Comparative analysis of activation induced marker (AIM) assays for sensitive identification of antigen-specific CD4 T cells. PLoS One *12*, e0186998. https://doi.org/10.1371/journal.pone.0186998.

43. Chakraborty, S., Gonzalez, J.C., Sievers, B.L., Mallajosyula, V., Chakraborty, S., Dubey, M., Ashraf, U., Cheng, B.Y.-L., Kathale, N., Tran, K.Q.T., et al. (2022). Early non-neutralizing, afucosylated antibody responses are associated with COVID-19 severity. Sci. Transl. Med. *14*, eabm7853. https://doi.org/10.1126/scitranslmed.abm7853.

44. Wei, J., Matthews, P.C., Stoesser, N., Maddox, T., Lorenzi, L., Studley, R., Bell, J.I., Newton, J.N., Farrar, J., Diamond, I., et al.; COVID-19 Infection Survey team (2021). Anti-spike antibody response to natural SARS-CoV-2 infection in the general population. Nat. Commun. *12*, 6250. https://doi.org/10.1038/s41467-021-26479-2.

45. Hu, Z., van der Ploeg, K., Chakraborty, S., Arunachalam, P., Mori, D.M., Jacobson, K.B., Bonilla, H., Parsonnet, J., Andrews, J., Hedlin, H., et al. (2021). Early immune responses have long-term associations with clinical, virologic, and immunologic outcomes in patients with COVID-19. Preprint at medRxiv. https://doi.org/10.1101/2021.08.27.21262687.

46. Menten, P., Proost, P., Struyf, S., Van Coillie, E., Put, W., Lenaerts, J.-P., Conings, R., Jaspar, J.-M., De Groote, D., Billiau, A., et al. (1999). Differential induction of monocyte chemotactic protein-3 in mononuclear leukocytes and fibroblasts by interferon-α/β and interferon-γ reveals MCP-3 heterogeneity. Eur. J. Immunol. *29*, 678–685. https://doi.org/10.1002/(sici)1521-4141(199902)29:02<678::aid-immu678>3.0.co;2-j.

47. Proost, P., Wuyts, A., and van Damme, J. (1996). Human monocyte chemotactic proteins-2 and -3: structural and functional comparison with MCP-1. J. Leukoc. Biol. *59*, 67–74. https://doi.org/10.1002/jlb.59.1.67.

48. Merad, M., and Martin, J.C. (2020). Pathological inflammation in patients with COVID-19: a key role for monocytes and macrophages. Nat. Rev. Immunol. *20*, 355–362. https://doi.org/10.1038/s41577-020-0331-4.

49. Yang, Y., Shen, C., Li, J., Yuan, J., Wei, J., Huang, F., Wang, F., Li, G., Li, Y., Xing, L., et al. (2020). Plasma IP-10 and MCP-3 levels are highly associated with disease severity and predict the progression of COVID-19. J. Allergy Clin. Immunol. *146*, 119–127.e4. https://doi.org/10.1016/j.jaci.2020.04.027.

50. Mateus, J., Dan, J.M., Zhang, Z., Rydyznski Moderbacher, C., Lammers, M., Goodwin, B., Sette, A., Crotty, S., and Weiskopf, D. (2021). Low-dose mRNA-1273 COVID-19 vaccine generates durable memory enhanced by cross-reactive T cells. Science *374*, eabj9853. https://doi.org/10.1126/science.abj9853.

51. Mulligan, M.J., Lyke, K.E., Kitchin, N., Absalon, J., Gurtman, A., Lockhart, S., Neuzil, K., Raabe, V., Bailey, R., Swanson, K.A., et al. (2020). Phase I/II study of COVID-19 RNA vaccine BNT162b1 in adults. Nature *586*, 589–593. https://doi.org/10.1038/s41586-020-2639-4.

52. Sahin, U., Muik, A., Derhovanessian, E., Vogler, I., Kranz, L.M., Vormehr, M., Baum, A., Pascal, K., Quandt, J., Maurus, D., et al. (2020). COVID-19 vaccine BNT162b1 elicits human antibody and TH1 T cell responses. Nature *586*, 594–599. https://doi.org/10.1038/s41586-020-2814-7.

53. Woldemeskel, B.A., Garliss, C.C., and Blankson, J.N. (2021). SARS-CoV-2 mRNA vaccines induce broad CD4+ T cell responses that recognize SARS-CoV-2 variants and HCoV-NL63. J. Clin. Invest. *131*, e149335. https://doi.org/10.1172/jci149335.

54. Betts, M.R., Nason, M.C., West, S.M., De Rosa, S.C., Migueles, S.A., Abraham, J., Lederman, M.M., Benito, J.M., Goepfert, P.A., Connors, M., et al. (2006). HIV nonprogressors preferentially maintain highly functional HIV-specific CD8+ T cells. Blood *107*, 4781–4789. https://doi.org/10.1182/blood-2005-12-4818.

55. Lin, L., Finak, G., Ushey, K., Seshadri, C., Hawn, T.R., Frahm, N., Scriba, T.J., Mahomed, H., Hanekom, W., Bart, P.-A., et al. (2015). COMPASS identifies T-cell subsets correlated with clinical outcomes. Nat. Biotechnol. *33*, 610–616. https://doi.org/10.1038/nbt.3187.

56. Murugesan, K., Jagannathan, P., Pham, T.D., Pandey, S., Bonilla, H.F., Jacobson, K., Parsonnet, J., Andrews, J.R., Weiskopf, D., Sette, A., et al. (2021). Interferon-γ release assay for accurate detection of severe acute respiratory syndrome coronavirus 2 T-cell response. Clin. Infect. Dis. *73*, e3130–e3132. https://doi.org/10.1093/cid/ciaa1537.

57. Tan, A.T., Lim, J.M.E., Le Bert, N., Bert, N.L., Kunasegaran, K., Chia, A., Qui, M.D.C., Tan, N., Chia, W.N., de Alwis, R., et al. (2021). Rapid measurement of SARS-CoV-2 spike T cells in whole blood from vaccinated and naturally infected individuals. J. Clin. Invest. *131*. https://doi.org/10.1172/jci152379.

58. Lönnberg, T., Svensson, V., James, K.R., Fernandez-Ruiz, D., Sebina, I., Montandon, R., Soon, M.S.F., Fogg, L.G., Nair, A.S., Liligeto, U.N., et al. (2017). Single-cell RNA-seq and computational analysis using temporal mixture modeling resolves T_H1/T_{FH} fate bifurcation in malaria. Sci. Immunol. *2*, eaal2192. https://doi.org/10.1126/sciimmunol.aal2192.

59. Jagannathan, P., Eccles-James, I., Bowen, K., Nankya, F., Auma, A., Wamala, S., Ebusu, C., Muhindo, M.K., Arinaitwe, E., Briggs, J., et al. (2014). IFNγ/IL-10 Co-producing cells dominate the CD4 response to malaria in highly exposed children. PLoS Pathog. *10*, e1003864. https://doi.org/10.1371/journal.ppat.1003864.

60. Ni, L., Ye, F., Cheng, M.-L., Feng, Y., Deng, Y.-Q., Zhao, H., Wei, P., Ge, J., Gou, M., Li, X., et al. (2020). Detection of SARS-CoV-2-specific humoral and cellular immunity in COVID-19 convalescent individuals. Immunity *52*, 971–977.e3. https://doi.org/10.1016/j.immuni.2020.04.023.

61. Arunachalam, P.S., Scott, M.K.D., Hagan, T., Li, C., Feng, Y., Wimmers, F., Grigoryan, L., Trisal, M., Edara, V.V., Lai, L., et al. (2021). Systems vaccinology of the BNT162b2 mRNA vaccine in humans. Nature *596*, 410–416. https://doi.org/10.1038/s41586-021-03791-x.

62. Keeton, R., Tincho, M.B., Ngomti, A., Baguma, R., Benede, N., Suzuki, A., Khan, K., Cele, S., Bernstein, M., Karim, F., et al. (2022). T cell responses to SARS-CoV-2 spike cross-recognize Omicron. Nature *603*, 488–492. https://doi.org/10.1038/s41586-022-04460-3.

63. Tarke, A., Coelho, C.H., Zhang, Z., Dan, J.M., Yu, E.D., Methot, N., Bloom, N.I., Goodwin, B., Phillips, E., Mallal, S., et al. (2022). SARS-CoV-2 vaccination induces immunological T cell memory able to cross-recognize variants from Alpha to Omicron. Cell *185*, 847–859.e11. https://doi.org/10.1016/j.cell.2022.01.015.

64. Bray, N.L., Pimentel, H., Melsted, P., and Pachter, L. (2016). Near-optimal probabilistic RNA-seq quantification. Nat. Biotechnol. *34*, 525–527. https://doi.org/10.1038/nbt.3519.

65. Korotkevich, G., Sukhov, V., Budin, N., Shpak, B., Artyomov, M.N., and Sergushichev, A. (2021). Fast gene set enrichment analysis. Preprint at bioRxiv. https://doi.org/10.1101/060012.

66. Roederer, M., Nozzi, J.L., and Nason, M.C. (2011). SPICE: exploration and analysis of post-cytometric complex multivariate datasets. Cytometry A *79*, 167–174. https://doi.org/10.1002/cyto.a.21015.

STAR★METHODS

KEY RESOURCES TABLE

REAGENT or RESOURCE	SOURCE	IDENTIFIER
Antibodies		
Mouse Anti-Human CCR7/BV421 (Clone: G043H7)	BioLegend	Cat# 353208; RRID: AB_11203894
Mouse Anti-Human CD14/BV510 (Clone: M5E2)	BioLegend	Cat# 301842; RRID: AB_2561946
Mouse Anti-Human CD19/BV510 (Clone: HB19)	BioLegend	Cat# 302242; RRID: AB_2561668
Mouse Anti-Human CD45RA/BV605 (Clone: HI100)	BioLegend	Cat# 304134; RRID: AB_2563814
Mouse Anti-Human CD4/BV650 (Clone: RPA-T4)	BioLegend	Cat# 300536; RRID: AB_2632791
Mouse Anti-Human CD8A/BV785 (Clone: RPA-T8)	BioLegend	Cat# 301046; RRID: AB_2563264
Mouse Anti-Human CD107A/FITC (Clone: H4A3)	BioLegend	Cat# 328606; RRID: AB_1186036
Mouse Anti-Human CD3/APC-H7 (Clone: SK7)	BD Biosciences	Cat# 560176; RRID: AB_1645475
Mouse Anti-Human IFNγ/PerCP Cy5.5 (Clone: 4S.B3)	BioLegend	Cat# 502526; RRID: AB_961355
Mouse Anti-Human IL21/eFluor660 (Clone: eBio3A3-N2)	eBioscience	Cat# 50-7219-42; RRID: AB_10598202
Mouse Anti-Human TNF/AF700 (Clone: MAb11)	BD Biosciences	Cat# 557996; RRID: AB_396978
Rat Anti-Human IL2/PE (Clone: MQ1-17H12)	BioLegend	Cat# 500307; RRID: AB_315094
Rat Anti-Human IL10/PE (Clone: JES3-19F1)	BD Biosciences	Cat# 559330; RRID: AB_397227
Mouse Anti-Human PD-1/BV421 (Clone: EH12.2H7)	BioLegend	Cat# 329920; RRID: AB_10960742
Mouse Anti-Human CXCR5/BV711 (Clone: J252D4)	BioLegend	Cat# 356934; RRID: AB_2629526
Mouse Anti-Human CD69/FITC (Clone: FN50)	BD Biosciences	Cat# 555530; RRID: AB_395915
Mouse Anti-Human OX40/PE (Clone: Ber-ACT35)	BioLegend	Cat# 350004; RRID: AB_10645478
Mouse Anti-Human CD137/APC (Clone: 4B4-1)	BioLegend	Cat# 309809; RRID: AB_830671
Mouse Anti-Human CD3/AF700 (Clone: SK7)	BioLegend	Cat# 344821; RRID: AB_2563419
Armenian Hamster Anti-Human ICOS/APC-Cy7 (Clone: C398.4A)	BioLegend	Cat# 313530; RRID: AB_2566128
LIVE/DEAD™ Fixable Aqua Dead Cell Stain	Invitrogen	Cat# L34965
Goat anti-Human IgG/HRP	Southern Biotech	Cat# 2040-05; RRID: AB_2795644
Bacterial and virus strains		
SARS-CoV-2 pseudoparticles	Chakraborty et al.	N/A
Chemicals, peptides, and recombinant proteins		
PepTivator® SARS-CoV-2 Prot_S	Miltenyi Biotec	Cat# 130-126-701
PepTivator® SARS-CoV-2 Prot_S1	Miltenyi Biotec	Cat# 130-127-048

(*Continued on next page*)

Continued

REAGENT or RESOURCE	SOURCE	IDENTIFIER
PepTivator® SARS-CoV-2 Prot_N	Miltenyi Biotec	Cat# 130-126-699
PepTivator® SARS-CoV-2 Prot_M	Miltenyi Biotec	Cat# 130-126-703
Critical commercial assays		
FIX & PERM® Cell Permeabilization Kit	Invitrogen	Cat# GAS004
Quick-RNA MagBead Kit	Zymo Research	Cat# R2132
Zymo-Seq Ribo-Free Total RNA Library Kit	Zymo Research	Cat# R3000
Deposited data		
RNA Sequencing data	Hu et al., 2021,[45] This paper	GEO: GSE178967
Proteomics data (Olink)	Hu et al., 2021,[45] This paper	https://github.com/hzc363/COVID19_system_immunology
Experimental models: Cell lines		
Vero cells	ATCC	Cat# CCL-81; RRID: CVCL_0059
Software and algorithms		
Prism 9	GraphPad	https://www.graphpad.com/
STATA	StataCorp LLC	https://www.stata.com/
SPICE	NIAID, Roederer et al.	https://niaid.github.io/spice/
RStudio	RStudio	https://www.rstudio.com/products/rstudio/
FlowJo	Becton Dickinson & Company	https://www.flowjo.com/solutions/flowjo
Kallisto	Bray et al., 2016[64]	https://github.com/pachterlab/kallisto
Ensembl	E!Ensembl	http://uswest.ensembl.org/index.html
Other		
Attune NXT Flow cytometer	Invitrogen	https://www.thermofisher.com/us/en/home/life-science/cell-analysis/flow-cytometry/flow-cytometers/attune-nxt-flow-cytometer/models/nxt.html
iD5 SPECTRAmax	Molecular devices	https://www.moleculardevices.com/products/microplate-readers/multi-mode-readers/spectramax-id3-id5-readers
Celigo Image Cytometer	Nexcelom Bioscience	https://www.nexcelom.com/nexcelom-products/cellometer-and-celigo-image-cytometers/celigo-imaging-cytometer/
NovaSeq 6000, S4	Illumina	https://www.illumina.com/systems/sequencing-platforms/novaseq.html
Whole blood transcriptomics	Novogene Corporation, Inc	https://en.novogene.com/
Plasma proteomics: Olink multiplex proximity extension assay (PEA) inflammation panel and immune response panel	Olink proteomics	https://www.olink.com/

RESOURCE AVAILABILITY

Lead contact

Further information and requests for resources and reagents should be directed to and will be fulfilled by the lead contact, Prasanna Jagannathan (prasj@stanford.edu).

Materials availability

This study did not generate new unique reagents.

Data and code availability

- RNA sequencing data have been deposited at NCBI Gene Expression Omnibus and are publicly available as of the date of publication. The accession number is listed in the key resources table.
- The Olink, clinical, virological, and immunological data, as well as the source codes, have been deposited the GitHub repository and are publicly available as of the date of publication. The GitHub link is listed in the key resources table.
- Additional supplemental items are available from Mendeley Data: https://doi.org/10.17632/nzd3f5c3j4.1.
- Other underlying data for this paper will be shared by the lead contact upon request without restriction.

EXPERIMENTAL MODEL AND SUBJECT DETAILS

Clinical cohort and human samples

The samples used were from 109 participants enrolled in a Phase 2, single-blind, randomized placebo-controlled trial evaluating the efficacy of Peginterferon Lambda-1a in SARS-CoV-2 infected outpatients.[40] The trial was registered at ClinicalTrials.gov (NCT04331899) and was performed as an investigator-initiated clinical trial with the FDA (IND 419217). In brief, symptomatic outpatients aged 18–71 who tested positive for reverse transcription-polymerase chain reaction (RT-PCR) detection of SARS-CoV-2 within 72 h of enrollment were eligible to participate in the study barring any signs of respiratory distress. Asymptomatic patients were eligible if they had not previously had a positive SARS-CoV-2 test. Full eligibility and exclusion criteria are provided in the study protocol and have been published.[40] On the day of enrollment, participants were randomized 1:1 to receive a single subcutaneous injection of Lambda or saline placebo. For the clinical trial, participants were followed for 28 days with an at home daily symptom survey (REDCap Cloud) and daily in-home assessments of temperature and oxygen saturation. In-person follow-up visits were conducted on day 1, 3, 5, 7, 10, 14, 21, 28 for symptom assessments, collection of oropharyngeal swabs, safety labs (day 5, 14), and peripheral blood biobanking (day 5, 14, 28). Participant baseline demographics and clinical characteristics are depicted in Table S1. Participants were invited to return for long-term follow-up visits at month four, month seven and month ten post-enrollment for a symptom survey, clinical assessment, assessment of vaccination status, and peripheral blood biobanking. Overall, 20 participants received 2 doses of COVID-19 mRNA vaccine before month seven (n = 2) or month ten (n = 18) follow-up visits (median 30 days since second dose at time of sampling, range 6–78). We also collected blood and serum samples from healthy volunteers, without known SARS-CoV-2 exposure, aged 22–35 to serve as our non-exposed controls. All participants gave written informed consent. The study protocol used was approved by the Institutional Review Board of Stanford University.

Viruses and cell lines

The generation of vesicular stomatitis virus (VSV) pseudo-typed with the S of SARS-CoV-2 used in the neutralization assays to infect Vero cells (ATCC, CCL-81) were made as described previously.[43] Vero cells are derived from an adult African green monkey. The sex of the cells is unknown because it is not specified by ATCC. Cells were grown and maintained in 1× Dulbecco's modified Eagle medium (Thermo Fisher Scientific) supplemented with 10% fetal bovine serum (FBS).

METHOD DETAILS

PBMC/serum isolation

Blood was collected from study participants in two BD Vacutainer® CPT™ Mononuclear Cell Preparation Tubes, which provide a fully-closed system for separation of mononuclear cells from whole blood. The tubes were centrifuged at 1800 g for 20 min, following centrifugation plasma was separated into a 15 mL centrifuge tube, centrifuged again at 1200 g for 10 min, then aliquot and stored at −80°C. The PBMC layer was transferred to a 50 mL centrifuge tube, washed twice with Gibco DPBS and centrifuged at 300 g for 10 min. After counting, the cells were aliquoted in 90% Fetal Bovine Serum and 10% DMSO at 5 million cells per vial. PBMC vials were stored overnight at −80°C, then transferred to liquid nitrogen storage. Whole blood was collected in Paxgene Tubes.

SARS-CoV-2 peptides

For *in vitro* stimulation experiments, we used PepTivator® SARS-CoV-2 lyophilized peptide pools from Miltenyi Biotec. We used Prot_M and Prot_N, consisting of complete sequences of the membrane 'M' glycoprotein (GenBank: MN908947.3, Protein QHD43419.1) and nucleocapsid 'N' phosphoprotein (GenBank: MN908947.3, Protein QHD43423.2) of SARS-CoV-2. For the spike 'S' glycoprotein of SARS-CoV-2 we used the combination of Prot_S1 and Prot_S peptide pools, which covers the aa sequence 1–692 of the N-terminal S1 domain (GenBank: MN908947.3, Protein QHD43416.1) and the immunodominant sequence domains, within aa 304–1273, of the S protein (GenBank: MN908947.3, Protein QHD43416.1), respectively.

Intracellular cytokine staining (ICS) assay

After thawing, PBMCs were rested overnight in complete RPMI (RPMI (Corning) supplemented with 10% FBS (Gibco), 100 IU Penicillin (Corning), 100 μg/mL Streptomycin (Corning), 1 mM Hepes (Corning) and 2 mM L-glutamine (Corning)). We prepared 96-well U-bottom plates with 1 × 10^6 cells in 200 μL of complete RPMI and then rested overnight at 37°C in a CO2 incubator. Cells

were cultured in presence of either SARS-CoV-2 peptides (1 μg/mL), PMA (300 ng/mL) and Ionomycin (1.5 μg/mL) as positive control, or media as a negative control for 6 h at 37°C the following morning. Brefeldin A (BD Pharmingen), Monensin (BD Pharmingen) and CD107a were present in all conditions from the start of incubation. Thereafter, cells were washed and surface stained for CCR7 for 15 min at 37°C, which was followed by the remaining surface stain for 30 min at room temperature (RT) in the dark. Afterwards, cells were washed twice with PBS containing 0.5% BSA and 2 mM EDTA, then fixed/permeabilized (FIX & PERM® Cell Permeabilization Kit, Invitrogen) and stained with intracellular antibodies for 20 min at RT in the dark. A complete list of antibodies is listed in Key resources table. Dilutions of antibodies used: BV421 CCR7 1/20; BV510 CD14 1/100; BV510 CD19 1/100; BV605 CD45RA 1/125; BV650 CD4 1/50; BV785 CD8A 1/50; FITC CD107A 1/50; APC-H7 CD3 1/20; PerCP Cy5.5 IFNγ 1/100; eFlour660 IL21 1/50; AF700 TNF 1/100; PE IL2 1/25; PE IL10 1/25 and Live/Dead Aqua 1:200.

Activation induced marker (AIM) assay

Thawed PBMCs were prepared in 96-well U-bottom plates at 1 × 10^6 cells, in 200 μL of complete RPMI and rested for 1 h at 37°C. The cells were stimulated overnight in presence of either SARS-CoV-2 peptides (1 μg/mL), PHA (2 μg/mL) as positive control, or media as a negative control at 37°C. Thereafter, cells were washed and surface stained for CXCR5 for 30 min at 37°C. This was followed by the remaining surface stain for 30 min at RT in the dark. Antibodies used are listed in key resources table. Dilutions of antibodies used: BV421 PD-1 1/25; BV510 CD14 1/100; BV510 CD19 1/100; BV605 CD45RA 1/125; BV650 CD4 1/50; BV711 CXCR5 1/50; BV785 CD8A 1/50; FITC CD69 1/40; PE OX40 1/20; APC CD137 1/20; AF700 CD3 1/50; APC-Cy7 ICOS 1/62.5 and Live/Dead Aqua 1:200. All samples were analyzed on an Attune NXT flow cytometer and analyzed with FlowJo 10 software (v10.8.0) (BD).

ELISA and neutralizing assay

ELISA and neutralizing assay were performed as described in detail previously.[43] In brief, IgG antibody titers against the SARS-CoV-2 spike receptor binding domain (RBD) were assessed at enrollment, day 28 and 210 post-enrollment by ELISA. Briefly, 96 Well Half-Area microplates (Corning (Millipore Sigma)) plates were coated with antigens at 2 μg/mL in PBS for 1 h at RT. Next, the plates were blocked and plasma was diluted 5-fold starting at 1:50, before adding 25 μL of the diluted plasma to each well and incubated for 2 h at RT. This is followed by adding 25 μL of 1:5000 diluted horseradish peroxidase (HRP) conjugated anti-Human IgG secondary antibodies (Southern Biotech) and incubated for 1 h at RT. The plates were developed and absorbance was measured at 450nm (iD5 SPECTRAmax, Molecular Devices).

In short, neutralization assays were performed by seeding Vero cells (ATCC CCL-81) 24 h prior to the assay and by plating patient plasma on a separate plate in serially 5-fold dilution, which was followed by adding 25 μL of SARS-CoV-2 pseudo-typed VSV particles to the wells on the dilution plate and incubated at 37°C for 1 h. Prior to infection, Vero cells were washed twice with 1X PBS and then 50 μL of the incubated pseudo-typed particles and patient plasma mixture was transferred onto the Vero cells, followed by a 24 h incubation at 37°C and 5% CO2. Afterwards, viral infection was analyzed by quantifying the number of GFP-expressing cells using a Celigo Image Cytometer (Nexcelom Bioscience).

Whole blood transcriptomics

Novogene Corporation, Inc. executed whole blood transcriptomics. In brief, using whole blood samples collected in Paxgene Tubes and treated with Proteinase K, RNA extraction was done using Quick-RNA MagBead Kit on KingFisher. Thereafter, quality control checks were performed using a Qubit and Bioanalyzer 2100. Libraries were prepared using ZymoSeq Ribo-Free Total RNA Library Kit and sequencing took place on a NovaSeq 6000 (Illumina) on an S4 lane, 30M paired reads, PE 150.

Plasma proteomics using olink panels

Proteins in plasma were measured using Olink multiplex proximity extension assay (PEA) inflammation panel and immune response panel (Olink proteomics, www.olink.com) according to the manufacturer's instructions and described by Hu et al.[45]

QUANTIFICATION AND STATISTICAL ANALYSIS

ELISA and neutralizing assay analysis

IgG antibody data obtained by ELISA were normalized between the same positive and negative controls and the binding area under the curve (AUC) reported.

In the neutralizing assay the percent infection was calculated based on the 'virus only' controls and then the percent inhibition was determined by subtracting the percent infection from 100. A non-linear curve and the half-maximal neutralization titer (NT50) were generated using Prism 9 (GraphPad).

Whole blood transcriptome data analysis

Using Kallisto (v0.46.2)[64] the transcript-level count data and transcript per million (TPM) data were calculated. Human cDNA index was produced using Kallisto on Ensembl (v96) transcriptomes. All gene ontology terms that are the child term of immune system process were identified (GO: 0002376). Highly redundant gene ontology terms by grouping terms with >80% overlap of genes were removed, followed by manually selecting the representative terms within each group. The single-sample enrichment score of

each gene ontology term was calculated for each RNA-seq sample by using the fgsea R package.[65] Gene ontology term enrichment scores were treated as variables, similar to individual protein markers, in downstream analysis.

T cell data and association analysis

All statistical analyses were performed using Prism 9 (v9.3.1) (GraphPad), STATA (v16) (StataCrop LLC), SPICE (v6.1) (NIAID),[66] and/or RStudio (v1.3.1093) (RStudio). Detailed statistical parameters are reported in the figure legends. Pie charts were generated using SPICE, heatmaps and association scatterplots were generated by using ggplot2 and tidyverse packages in RStudio, and all other graphs were made in Prism 9.

Percentages of SARS-CoV-2-specific cytokine producing T cells (alone or in combination) are reported after background subtraction of the percentage of the identically gated population of cells from the same sample stimulated with media control. Background-subtracted responses were considered positive if >0.01% parent population. Samples included in experiments with poor or no viability (determined by Live/Dead Aqua stain (Invitrogen)) were excluded during analysis. Age categories were defined by participant age quartiles. Comparisons of cytokine percentages between groups were done using the Mann Whitney test. The Wilcoxon matched-pairs signed-rank test or Friedman test with Dunn's multiple comparison test were used to compare paired data. Statistical analyses of global cytokine profiles (pie charts) were performed by partial permutation tests using SPICE. Continuous variables were compared using Spearman correlation with Benjamini-Hochberg multiple comparison correction. For multivariate linear regression models, non-normal variables were log-transformed. Linear regression was used to estimate associations between T cell responses measured on day 28 and neutralizing antibody levels measured on month four, adjusting for participant sex, treatment arm, and age.

We tested associations between plasma proteins measured by Olink, whole blood transcriptomics, and $CD4^+$ T cell responses using regression models and the lm function in R, adjusting for time since symptom onset and the stimulation type (MN or S) of the T cell response (T cell responses $\sim$ measurements + Stim + time + time).[2] Both the first and second order term of time were included in the model to adjust for the non-linear relationship between time and immune response, as described in an early publication.[45] The p value of the regression coefficient of the measurement term is used to determine the significance of association between T cell response and the immune measurements. The False Discovery Rate (FDR) method is used to adjust for the multiple hypothesis testings when assessing the association between T cell response and the immune measures (plasma proteins and immune pathways).

Two-sided p-values were calculated for all test statistics and $p < 0.05$ was considered significant.

ADDITIONAL RESOURCES

Clinical trial: https://clinicaltrials.gov/ct2/show/NCT04331899.